

PhD Thesis "Flatness-based Constrained Control
and Model-Free Control Applications to
Quadrotors and Cloud Computing"

Chapter 2: Constraints on Nonlinear Finite
Dimensional Flat Systems

Author: Maria Bekcheva

July 2019

PhD directors: Hugues Mounier and Luca Greco
Université Paris-Saclay

This is the second chapter in my thesis "Flatness-based Constrained Control
and Model-Free Control Applications to Quadrotors and Cloud Computing".
Comments and suggestions are most welcome ¹.

¹`maria.bekcheva@l2s.centralesupelec.fr` or `maria.bekcheva@gmail.com`.

Contents

1	Chapter overview	4
1.1	Motivation	4
1.2	Research objective and contribution	5
1.3	Existing Methods	7
1.4	Outline	7
2	Differential flatness overview	8
3	Problem statement: Trajectory constraints fulfilment	9
3.1	General problem formulation	9
3.2	Constraints in the flat output space	10
3.3	Problem specialisation	11
3.4	Closed-loop trajectory tracking	13
4	Preliminaries on Symbolic Bézier trajectory	14
4.1	Definition of the Bézier curve	15
4.2	Bézier properties	15
4.3	Quantitative envelopes for the Bézier curve	17
4.4	Symbolic Bézier operations	18
4.5	Bézier time derivatives	19
5	Constrained feedforward trajectory procedure	23
6	Feasible control points regions	24
6.1	Cylindrical Algebraic Decomposition	26
6.2	Approximations of Semialgebraic Sets	27
7	Applications	29
7.1	Longitudinal dynamics of a vehicle	29
7.1.1	Symbolic input constraints	30
7.1.2	Simulation results	32
7.2	Quadrotor dynamics	33
7.2.1	Motivation	33
7.2.2	Simplified model of quadrotor	35
7.2.3	Differential flatness of the quadrotor	35
7.2.4	Constraints	36
7.2.5	Constrained open-loop trajectory u_{1r}	37
7.2.6	Constrained open-loop trajectories θ_r et ϕ_r	38
7.2.7	Constrained open-loop trajectories x_r and y_r	42
7.2.8	Constrained open-loop trajectories u_2 and u_3	43
7.2.9	Constrained open-loop control for u_{4r}	43
8	Closing remarks	44
A	Geometrical signification of the Bezier operations	46

Abstract: This chapter presents an approach to embed the input/state/output constraints in a unified manner into the trajectory design for differentially flat systems. To that purpose, we specialize the flat outputs (or the reference trajectories) as Bézier curves. Using the flatness property, the system's inputs/states can be expressed as a combination of Bézier curved flat outputs and their derivatives. Consequently, we explicitly obtain the expressions of the control points of the inputs/states Bézier curves as a combination of the control points of the flat outputs. By applying desired constraints to the latter control points, we find the feasible regions for the output Bézier control points i.e. a set of feasible reference trajectories.

1 Chapter overview

1.1 Motivation

The control of nonlinear systems subject to *state and input constraints* is one of the major challenges in control theory. Traditionally, in the control theory literature, the reference trajectory to be tracked is specified in advance. Moreover for some applications, for instance, the quadrotor trajectory tracking, selecting the *right trajectory* in order to avoid obstacles while not damaging the actuators is of crucial importance.

In the last few decades, Model Predictive Control (MPC) [7, 37] has achieved a big success in dealing with constrained control systems. Model predictive control is a form of control in which the current control law is obtained by solving, at each sampling instant, a finite horizon open-loop optimal control problem, using the current state of the system as the initial state; the optimization yields an optimal control sequence and the first control in this sequence is applied to the system. It has been widely applied in petro-chemical and related industries where satisfaction of constraints is particularly important because efficiency demands operating points on or close to the boundary of the set of admissible states and controls.

The optimal control or MPC maximize or minimize a defined performance criterion chosen by the user. The optimal control techniques, even in the case without constraints are usually discontinuous, which makes them less robust and more dependent of the initial conditions. In practice, this means that the delay formulation renders the numerical computation of the optimal solutions difficult.

A large part of the literature working on constrained control problems is focused on optimal trajectory generation [16, 31]. These studies are trying to find feasible trajectories that optimize the performance following a specified criterion. Defining the right criterion to optimize may be a difficult problem in practice. Usually, in such cases, the feasible and the optimal trajectory are not too much different. For example, in the case of autonomous vehicles [29], due to the dynamics, limited curvature, and under-actuation, a vehicle often has few options for how it changes lanes on highways or how it travels over the space

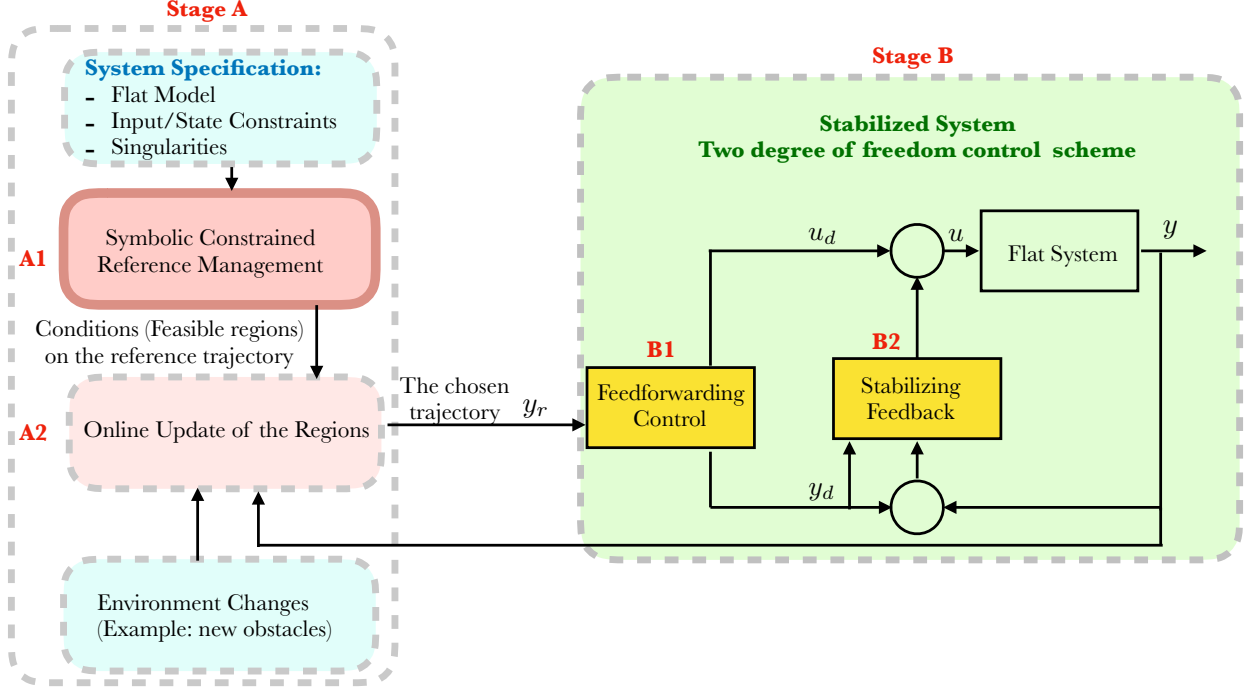


Figure 1: Two degrees of freedom control scheme overview

immediately in front of it. Regarding the complexity of the problem, searching for a feasible trajectory is *easier*, especially in the case where we need *real-time re-planning* [26, 27]. Considering that the evolution of transistor technologies is reaching its limits, low-complexity controllers that can take the constraints into account are of considerable interest. The same remark is valid when the system has sensors with limited performance.

1.2 Research objective and contribution

In this chapter, we propose a novel trajectory-based framework to deal with system constraints. We are answering the following question:

Question 1 *How to design a set of the reference trajectories (or the feed-forwarding trajectories) of a nonlinear system such that the input, state and/or output constraints are fulfilled?*

For that purpose, we divide the control problem in two stages (see Figure 1). Our objective will be to elaborate a *constrained reference trajectory management* (Stage A) which is meant to be applied to already pre-stabilized systems (Stage B).

Unlike other receding horizon approaches which attempt to solve stabilization, tracking, and constraint fulfilment at the same time, we assume that in *Stage B*, a primal controller has already been designed to stabilize the system which provide nice tracking properties in the absence of constraints. In stage B, we employ the two-degree of freedom design consisting of a constrained trajectory design (constrained feedforwarding) and a feedback control.

In *Stage A*, the constraints are embedded in the flat output trajectory design. Thus, *our constrained trajectory generator* defines a feasible open-loop reference trajectory satisfying the states and/or control constraints that *a primal feedback controller* will track and stabilize around.

To construct Stage A we first take advantage of the *differential flatness property* which serves as a base to construct our method. The differential flatness property yields exact expressions for the state and input trajectories of the system through trajectories of a flat output and its derivatives without integrating any differential equation. The latter property allows us to map the state/input constraints into the flat output trajectory space.

Then, in our symbolic approach (stage A1), we assign a Bézier curve to each flat output where the parameter to be chosen are the so-called *control points* (yielding a finite number of variables on a finite time horizon) given in a symbolic form. This kind of representation naturally offers several algebraic operations like the sum, the difference and multiplication, and affords us to preserve the explicit functions structure without employing discrete numerical methods. The advantage to deal with the constraints *symbolically*, rather than numerically, lies in that the symbolic solution explicitly depends on the control points of the reference trajectory. This allows to study how the input or state trajectories are influenced by the reference trajectory.

We find symbolic conditions on the trajectory control points such that the states/inputs constraints are fulfilled.

We translate the state/input constraints into constraints on the reference trajectory control points and we wish to reduce the solution of the systems of equations/inequations into a simpler one. Ideally, we want to find the exact set of solutions *i.e.* the constrained subspace.

We explain how this symbolic constrained subspace representation can be used for *constrained feedforwarding trajectory selection*. The stage A2 can be done in two different ways.

- When a system should track a trajectory in a *static known environment*, then the exact set of feasible trajectories is found and the trajectory is fixed by our choice. If the system's environment changes, we only need to re-evaluate the exact symbolic solution with new numerical values.
- When a system should track a trajectory in an *unknown environment with moving objects*, then, whenever necessary, the reference design modifies the reference supplied to a primal control system so as to enforce the fulfilment of the constraints. This second problem is not addressed in the thesis.

Our approach is *not based on any kind of optimization* nor does it need com-

putations for a given numerical value at each sampling step. We determine a set of feasible trajectories through the system constrained environment that enable a controller to make quick real-time decisions. For systems with singularities, we can isolate the singularities of the system by considering them as additional constraints.

1.3 Existing Methods

- Considering actuator constraints based on the derivatives of the flat output (for instance, the jerk [22, 53], snap [38]) can be too conservative for some systems. The fact that a feasible reference trajectory is designed following the system model structure allows to choose a quite aggressive reference trajectory.
- In contrast to [51], we characterize the whose set of viable reference trajectories which take the constraints into account.
- In [47], the problem of constrained trajectory planning of differentially flat systems is cast into a simple quadratic programming problem ensuing computational advantages by using the flatness property and the B-splines curve's properties. They simplify the computation complexity by taking advantage of the B-spline minimal (resp. maximal) control point. The simplicity comes at the price of having only minimal (resp. maximal) constant constraints that eliminate the possible feasible trajectories and renders this approach conservative.
- In [23], an inversion-based design is presented, in which the transition task between two stationary set-points is solved as a two-point boundary value problem. In this approach, the trajectory is defined as polynomial where only the initial and final states can be fixed.
- The thesis of Bak [2] compared existing methods to constrained controller design (anti-windup, predictive control, nonlinear methods), and introduced a nonlinear gain scheduling approach to handle actuator constraints.

1.4 Outline

This chapter is organized as follows:

- In section 2, we recall the notions of differential flatness for finite dimensional systems.
- In section 3, we present our problem statement for the constraints fulfilment through the reference trajectory.
- In section 4, we detail the flat output parameterization given by the Bézier curve, and its properties.

- In section 5, we give the whole procedure in establishing reference trajectories for constrained open-loop control. We illustrate the procedure through two applications in section 7.
- In section 6, we present the two methods that we have used to compute the constrained set of feasible trajectories.

2 Differential flatness overview

The concept of *differential flatness* was introduced in [20, 19] for non-linear finite dimensional systems. By the means of differential flatness, a non-linear system can be seen as a controllable linear system through a dynamical feedback.

A model shall be described by a differential system as:

$$\dot{\mathbf{x}} = f(\mathbf{x}, \mathbf{u}) \quad (1)$$

where $\mathbf{x} \in \mathbb{R}^n$ denote the *state variables* and $\mathbf{u} \in \mathbb{R}^m$ the *input vector*. Such a system is said to be *flat* if there exists a set of *flat outputs* (or *linearizing outputs*) (equal in number to the number of inputs) given by

$$\mathbf{y} = h(\mathbf{x}, \mathbf{u}, \dot{\mathbf{u}}, \dots, \mathbf{u}^{(r)}) \quad (2)$$

with $r \in \mathbb{N}$ such that the components of $\mathbf{y} \in \mathbb{R}^m$ and all their derivatives are functionally independent and such that we can parametrize every solution (\mathbf{x}, \mathbf{u}) of (1) in some dense open set by means of the flat output \mathbf{y} and its derivatives up to a finite order q :

$$\mathbf{x} = \psi(\mathbf{y}, \dot{\mathbf{y}}, \dots, \mathbf{y}^{(q-1)}), \quad (3a)$$

$$\mathbf{u} = \zeta(\mathbf{y}, \dot{\mathbf{y}}, \dots, \mathbf{y}^{(q)}) \quad (3b)$$

where (ψ, ζ) are *smooth functions* that give the trajectories of \mathbf{x} and \mathbf{u} as functions of the flat outputs and their time derivatives. The preceding expressions in (3), will be used to obtain the so called *open-loop controls*. The differential flatness found numerous applications, non-holonomic systems, among others (see [45] and the references therein).

In the context of feedforwarding trajectories, the “degree of continuity” or the smoothness of the reference trajectory (or curve) is one of the most important factors. The smoothness of a trajectory is measured by the number of its continuous derivatives. We give the definitions on the trajectory continuity when it is represented by a parametric curve in the Appendix B.

3 Problem statement: Trajectory constraints fulfilment

Notation

Given the scalar function $z \in C^\kappa(\mathbb{R}, \mathbb{R})$ and the number $\alpha \in \mathbb{N}$, we denote by $\mathbf{z}^{(\alpha)}$ the tuple of derivatives of z up to the order $\alpha \leq \kappa$: $\mathbf{z}^{(\alpha)} = z, \dot{z}, \ddot{z}, \dots, z^{(\alpha)}$. Given the vector function $\mathbf{v} = (v_1, \dots, v_q)$, $v_i \in C^\kappa(\mathbb{R}, \mathbb{R})$ and the tuple $\boldsymbol{\alpha} = (\alpha_1, \dots, \alpha_q)$, $\alpha_i \in \mathbb{N}$, we denote by $\mathbf{v}^{(\boldsymbol{\alpha})}$ the tuple of derivatives of each component v_i of \mathbf{v} up to its respective order $\alpha_i \leq \kappa$: $\mathbf{v}^{(\boldsymbol{\alpha})} = v_1, \dots, v_1^{(\alpha_1)}, v_2, \dots, v_2^{(\alpha_2)}, \dots, v_q, \dots, v_q^{(\alpha_q)}$.

3.1 General problem formulation

Consider the nonlinear system

$$\dot{\mathbf{x}}(t) = f(\mathbf{x}(t), \mathbf{u}(t)) \quad (4)$$

with state vector $\mathbf{x} = (x_1, \dots, x_n)$ and control input $\mathbf{u} = (u_1, \dots, u_m)$, $x_i, u_j \in C^\kappa([0, +\infty), \mathbb{R})$ for a suitable $\kappa \in \mathbb{N}$. We assume the state, the input and their derivatives to be subject to both inequality and equality constraints of the form

$$C_i(\mathbf{x}^{(\alpha_i^x)}(t), \mathbf{u}^{(\alpha_i^u)}(t)) \leq 0 \quad \forall t \in [0, T], \forall i \in \{1, \dots, \nu^{\text{in}}\} \quad (5a)$$

$$D_j(\mathbf{x}^{(\beta_j^x)}(t), \mathbf{u}^{(\beta_j^u)}(t)) = 0 \quad \forall t \in I_j, \forall j \in \{1, \dots, \nu^{\text{eq}}\} \quad (5b)$$

with each I_j being either $[0, T]$ (continuous equality constraint) or a discrete set $\{t_1, \dots, t_\gamma\}$, $0 \leq t_1 \leq \dots \leq t_\gamma \leq T < +\infty$ (discrete equality constraint), and $\alpha_i^x, \beta_j^x \in \mathbb{N}^n$, $\alpha_i^u, \beta_j^u \in \mathbb{N}^m$. We stress that the relations (5) specify objectives (and constraints) on the finite interval $[0, T]$. Objectives can be also formulated as a concatenation of sub-objectives on a union of sub-intervals, provided that some continuity and/or regularity constraints are imposed on the boundaries of each sub-interval. Here we focus on just one of such intervals.

Our aim is to characterise the set of input and state trajectories (\mathbf{x}, \mathbf{u}) satisfying the system's equations (4) and the constraints (5). More formally we state the following problem.

Problem 1 (Constrained trajectory set) *Let \mathcal{C} be a subspace of $C^\kappa([0, +\infty), \mathbb{R})$. Constructively characterise the set $\mathcal{C}^{\text{cons}} \subseteq \mathcal{C}^{n+m}$ of all extended trajectories (\mathbf{x}, \mathbf{u}) satisfying the system (4) and the constraints (5).*

Problem 1 can be considered as a generalisation of a constrained reachability problem (see for instance [17]). In such a reachability problem the stress is usually made on initial and final set-points and the goal is to find a suitable input to steer the state from the initial to the final point while possibly fulfilling the constraints. Here, we wish to give a functional characterisation of the overall set of extended trajectories (\mathbf{x}, \mathbf{u}) satisfying some given differential constraints. A classical constrained reachability problem can be cast in the present formalism

by limiting the constraints C_i and D_j to \mathbf{x} and \mathbf{u} (and not their derivatives) and by forcing two of the equality constraints to coincide with the initial and final set-points.

Problem 1 is difficult to be addressed in its general setting. To simplify the problem, in the following we make some restrictions to the class of systems and to the functional space \mathcal{C} . As a first assumption we limit the analysis to differentially flat systems [20].

3.2 Constraints in the flat output space

Let us assume that system (4) is differentially flat with flat output²

$$\mathbf{y} = (y_1, \dots, y_m) = h(\mathbf{x}, \mathbf{u}^{\langle \rho^u \rangle}), \quad (6)$$

with $\rho^u \in \mathbb{N}^m$. Following Equation (3), the parameterisation or the feedforward trajectories associated to the reference trajectory \mathbf{y}_r is

$$\mathbf{x}_r = \psi(\mathbf{y}_r^{\langle \eta^x \rangle}) \quad (7a)$$

$$\mathbf{u}_r = \zeta(\mathbf{y}_r^{\langle \eta^u \rangle}), \quad (7b)$$

with $\eta^x \in \mathbb{N}^n$ and $\eta^u \in \mathbb{N}^m$.

Through the first step of the dynamical extension algorithm [18], we get the flat output dynamics

$$\begin{cases} y_1^{(k_1)} = \phi_1(\mathbf{y}^{\langle \mu_1^y \rangle}, \mathbf{u}^{\langle \mu_1^u \rangle}) \\ \vdots \\ y_m^{(k_m)} = \phi_m(\mathbf{y}^{\langle \mu_m^y \rangle}, \mathbf{u}^{\langle \mu_m^u \rangle}), \end{cases} \quad (8)$$

with $\mu_i^y = (\mu_{i1}^y, \dots, \mu_{im}^y) \in \mathbb{N}^m$, $\mu_i^u = (\mu_{i1}^u, \dots, \mu_{im}^u) \in \mathbb{N}^m$ and $k_i > \max_j \mu_{ji}^y$. The original n -dimensional dynamics (4) and the K -dimensional flat output dynamics (8) ($K = \sum_i k_i$) are in one-to-one correspondence through (6) and (7). Therefore, the constraints (5) can be re-written as

$$\Gamma_i(\mathbf{y}_r^{\langle \omega_i^{\text{in}} \rangle}) \leq 0 \quad \forall t \in [0, T], \forall i \in \{1, \dots, \nu^{\text{in}}\} \quad (9a)$$

$$\Delta_j(\mathbf{y}_r^{\langle \omega_j^{\text{eq}} \rangle}) = 0 \quad \forall t \in I_j, \forall j \in \{1, \dots, \nu^{\text{eq}}\} \quad (9b)$$

with

$$\Gamma_i(\mathbf{y}_r^{\langle \omega_i^{\text{in}} \rangle}) = C_i((\psi(\mathbf{y}_r^{\langle \eta^x \rangle}))^{\langle \alpha_i^x \rangle}, \zeta(\mathbf{y}_r^{\langle \eta^u \rangle})^{\langle \alpha_i^u \rangle}),$$

$$\Delta_j(\mathbf{y}_r^{\langle \omega_j^{\text{eq}} \rangle}) = D_j((\psi(\mathbf{y}_r^{\langle \eta^x \rangle}))^{\langle \beta_j^x \rangle}, \zeta(\mathbf{y}_r^{\langle \eta^u \rangle})^{\langle \beta_j^u \rangle})$$

and $\omega_i^{\text{in}}, \omega_j^{\text{eq}} \in \mathbb{N}^m$.

²We recall that the flat output \mathbf{y} has the same dimension m as the input vector \mathbf{u} .

Remark 1 We may use the same result to embed an input rate constraint $\dot{\mathbf{u}}_r$.

Thus, Problem 1 can be transformed in terms of the flat output dynamics (8) and the constraints (9) as follows.

Problem 2 (Constrained flat output set) ³ Let \mathcal{C}_y be a subspace of $C^p([0, +\infty), \mathbb{R})$ with $p = \max((k_1, \dots, k_m), \omega_1^{\text{in}}, \dots, \omega_{\nu^{\text{in}}}^{\text{in}}, \omega_1^{\text{eq}}, \dots, \omega_{\nu^{\text{eq}}}^{\text{eq}})$. Constructively characterise the set $\mathcal{C}_y^{\text{cons}} \subseteq \mathcal{C}_y^m$ of all flat outputs satisfying the dynamics (8) and the constraints (9).

Working with differentially flat systems allows us to translate, in a unified fashion, all the state and input constraints as constraints in the flat outputs and their derivatives (See (9)). We remark that ψ and ζ in (7) are such that $\psi(\mathbf{y}^{(\eta_x)})$ and $\zeta(\mathbf{y}^{(\eta_u)})$ satisfy the dynamics of system (4) by construction. In other words, the extended trajectories (\mathbf{x}, \mathbf{u}) of (4) are in one-to-one correspondence with $\mathbf{y} \in \mathcal{C}_y^m$ given by (6). Hence, choosing \mathbf{y} solution of Problem 2 ensures that \mathbf{x} and \mathbf{u} given by (7) are solutions of Problem 1.

3.3 Problem specialisation

For any practical purpose, one has to choose the functional space \mathcal{C}_y to which all components of the flat output belong. Instead of making reference to the space $\mathcal{C}^{\text{gen}} := C^p([0, +\infty), \mathbb{R})$, mentioned in the statement of Problem 1, we focus on the space $\mathcal{C}_T^{\text{gen}} := C^p([0, T], \mathbb{R})$. Indeed, the constraints (9) specify finite-time objectives (and constraints) on the interval $[0, T]$. Still, the problem exhibits an infinite dimensional complexity, whose reduction leads to choose an approximation space \mathcal{C}^{app} that is dense in $\mathcal{C}_T^{\text{gen}}$. A possible choice is to work with parametric functions expressed in terms of basis functions like, for instance, Bernstein-Bézier, Chebychev or Spline polynomials.

A scalar Bézier curve of degree $N \in \mathbb{N}$ in the Euclidean space \mathbb{R} is defined as

$$P(s) = \sum_{j=0}^N \alpha_j B_{jN}(s), \quad s \in [0, 1]$$

where the $\alpha_j \in \mathbb{R}$ are the control points and $B_{jN}(s) = \binom{N}{j} (1-s)^{N-j} s^j$ are Bernstein polynomials [13]. For sake of simplicity, we set here $T = 1$ and we choose as functional space

$$\mathcal{C}^{\text{app}} = \left\{ \sum_0^N \alpha_j B_{jN} \mid N \in \mathbb{N}, (\alpha_j)_0^N \in \mathbb{R}^{N+1}, B_j \in \mathcal{C}^0([0, 1], \mathbb{R}) \right\} \quad (10)$$

The set of Bézier functions of generic degree has the very useful property of being closed with respect to addition, multiplication, degree elevation, derivation and integration operations (see section 4). As a consequence, any polynomial integro-differential operator applied to a Bézier curve, still produces a

³Here the max operator is applied elementwise on each vector.

Bézier curve (in general of different degree). Therefore, if the flat outputs \mathbf{y} are chosen in \mathcal{C}^{app} and the operators $\Gamma_i(\cdot)$ and $\Delta_j(\cdot)$ in (9) are integro-differential polynomials, then such constraints can still be expressed in terms of Bézier curves in \mathcal{C}^{app} . We stress that, if some constraints do not admit such a description, we can still approximate them up to a prefixed precision ε as function in \mathcal{C}^{app} by virtue of the denseness of \mathcal{C}^{app} in $\mathcal{C}_1^{\text{gen}}$. Hence we assume the following.

Assumption 1 *Considering each flat output $y_r \in \mathcal{C}^{\text{app}}$ defined as*

$$y_r = \sum_{j=0}^N \alpha_j B_{jN}(s),$$

the constraints (9) can be written as

$$\Gamma_i(\mathbf{y}_r^{\langle \omega_i^{\text{in}} \rangle}) = \sum_{k=0}^{N_i^{\text{in}}} \lambda_{ik} B_{kN}(s), \quad (11)$$

$$\Delta_j(\mathbf{y}_r^{\langle \omega_j^{\text{eq}} \rangle}) = \sum_{k=0}^{N_j^{\text{eq}}} \delta_{jk} B_{kN}(s) \quad (12)$$

where

$$\begin{aligned} \lambda_{ik} &= r_{ik}^{\text{in}}(\alpha_0, \dots, \alpha_N) \\ \delta_{jk} &= r_{jk}^{\text{eq}}(\alpha_0, \dots, \alpha_N) \\ r_{ik}^{\text{in}}, r_{jk}^{\text{eq}} &\in \mathbb{R}[\alpha_0, \dots, \alpha_N] \end{aligned}$$

i.e. the λ_{ik} and δ_{jk} are polynomials in the $\alpha_0, \dots, \alpha_N$. ■

Set the following expressions as ν^{in}

$$\begin{aligned} r^{\text{in}} &= (r_{1,0}^{\text{in}}, \dots, r_{\nu^{\text{in}}, N_{\nu^{\text{in}}}^{\text{in}}}^{\text{in}}), \\ r^{\text{eq}} &= (r_{1,0}^{\text{eq}}, \dots, r_{\nu^{\text{eq}}, N_{\nu^{\text{eq}}}^{\text{eq}}}^{\text{eq}}), \\ r &= (r^{\text{in}}, r^{\text{eq}}), \end{aligned}$$

the control point vector $\boldsymbol{\alpha} = (\alpha_1, \dots, \alpha_N)$, and the basis function vector $\mathbf{B} = (B_{1N}, \dots, B_{NN})$. Therefore, we obtain a semi-algebraic set defined as:

$$\mathcal{J}(r, \mathbb{A}) = \{ \boldsymbol{\alpha} \in \mathbb{A} \mid r^{\text{in}}(\boldsymbol{\alpha}) \leq 0, r^{\text{eq}}(\boldsymbol{\alpha}) = 0 \}$$

for any parallelotope

$$\mathbb{A} = [\underline{\alpha}_0, \bar{\alpha}_0] \times \dots \times [\underline{\alpha}_N, \bar{\alpha}_N], \underline{\alpha}_i, \bar{\alpha}_i \in \mathbb{R} \cup \{-\infty, \infty\}, \underline{\alpha}_i < \bar{\alpha}_i \quad (13)$$

Thus $\mathcal{J}(r, \mathbb{A})$ is a semi-algebraic set associated to the constraints (9). The parallelotope \mathbb{A} represents the trajectory sheaf of available trajectories, among which the user is allowed to choose a reference. The semi-algebraic set $\mathcal{J}(r, \mathbb{A})$

represents how the set \mathbb{A} is transformed in such a way that the trajectories fulfill the constraints (9). Then, picking an α in $\mathcal{J}(r, \mathbb{A})$ ensures that $y_r = \alpha B$ automatically satisfies the constraints (9).

The Problem 2 is then reformulated as :

Problem 3 *For any fixed parallelotope \mathbb{A} , constructively characterise the semi-algebraic set $\mathcal{J}(r, \mathbb{A})$.*

This may be done through exact, symbolic techniques (such as, *e.g.* the Cylindrical Algebraic Decomposition) or through approximation techniques yielding outer approximations $\mathcal{J}_l^{out}(r, \mathbb{A}) \supseteq \mathcal{J}(r, \mathbb{A})$ and inner approximations $\mathcal{J}_l^{inn}(r, \mathbb{A}) \subseteq \mathcal{J}(r, \mathbb{A})$ with $\lim_{l \rightarrow \infty} \mathcal{J}_l^{out} = \lim_{l \rightarrow \infty} \mathcal{J}_l^{inn} = \mathcal{J}$. ■

This characterisation shall be useful to extract inner approximations of a special type yielding trajectory sheaves included in $\mathcal{J}(r, \mathbb{A})$. A specific example of this type of approximations will consist in disjoint unions of parallelotopes:

$$\mathcal{J}_l^{inn}(r, \mathbb{A}) = \bigcup_{j \in I_l} \mathbb{B}_{l,j}, \quad \forall i, j \in I_l, \mathbb{B}_{l,i} \cap \mathbb{B}_{l,j} = \emptyset \quad (14)$$

This class of inner approximation is of practical importance for end users, as the applications in Section 7 illustrate.

3.4 Closed-loop trajectory tracking

So far this chapter has focused on the design of open-loop trajectories while assuming that the system model is perfectly known and that the initial conditions are exactly known. When the reference open-loop trajectories $(\mathbf{x}_r, \mathbf{u}_r)$ are well-designed *i.e.* respecting the constraints and avoiding the singularities, as discussed above, the system is close to the reference trajectory. However, to cope with the environmental disturbances and/or small model uncertainties, the tracking of the constrained open-loop trajectories should be made robust using *feedback control*. The feedback control guarantees the stability and a certain robustness of the approach, and is called the second degree of freedom of the primal controller (Stage B2 in figure 1).

We recall that some flat systems can be transformed via endogenous feedback and coordinate change to a linear dynamics [20, 45]. To make this chapter self-contained, we briefly discuss the *closed-loop trajectory tracking* as presented in [36].

Consider a differentially flat system with flat output $\mathbf{y} = (y_1, \dots, y_m)$ (m being the number of independent inputs of the system). Let $\mathbf{y}_r(t) \in C^\eta(\mathbb{R})$ be a reference trajectory for \mathbf{y} . Suppose the desired open-loop state/ input trajectories $(x_r(t), u_r(t))$ are generated offline. We need now a feedback control to track them.

Since the nominal open-loop control (or the feedforward input) linearizes the system, we can take a simple linear feedback, yielding the following closed-loop

error dynamics:

$$\mathbf{e}^{(\eta)} + \lambda_{\eta-1}\mathbf{e}^{(\eta-1)} + \dots + \lambda_1\dot{\mathbf{e}} + \lambda_0\mathbf{e} = 0 \quad (15)$$

where $\mathbf{e} = \mathbf{y} - \mathbf{y}_r$ is the tracking error and the coefficients $\Lambda = [\lambda_0, \dots, \lambda_{\eta-1}]$ are chosen to ensure an asymptotically stable behaviour (see e.g. [19]).

Remark 2 *Note that this is not true for all flat systems, in [24] can be found an example of flat system with nonlinear error dynamics.*

Now let (\mathbf{x}, \mathbf{u}) be the closed-loop trajectories of the system. These variables can be expressed in terms of the flat output \mathbf{y} as:

$$\mathbf{x} = \psi(\mathbf{y}^{\langle\eta-1\rangle}), \quad \mathbf{u} = \zeta(\mathbf{y}^{\langle\eta\rangle}) \quad (16)$$

Then, the associated reference open-loop trajectories $(\mathbf{x}_r, \mathbf{u}_r)$ are given by

$$\mathbf{x}_r = \psi(\mathbf{y}_r^{\langle\eta-1\rangle}), \quad \mathbf{u}_r = \zeta(\mathbf{y}_r^{\langle\eta\rangle})$$

Therefore,

$$\mathbf{x} = \psi(\mathbf{y}^{\langle\eta-1\rangle}) = \psi(\mathbf{y}_r^{\langle\eta-1\rangle} + \mathbf{e}^{\langle\eta-1\rangle})$$

and

$$\mathbf{u} = \zeta(\mathbf{y}^{\langle\eta\rangle}) = \zeta(\mathbf{y}_r^{\langle\eta\rangle} + \mathbf{e}^{\langle\eta\rangle}, -\Lambda\mathbf{e}^{\langle\eta\rangle}).$$

As further demonstrated in [36][See Section 3.3], since the tracking error $\mathbf{e} \rightarrow 0$ as $t \rightarrow \infty$ that means $\mathbf{x} \rightarrow \mathbf{x}_r$ and $\mathbf{u} \rightarrow \mathbf{u}_r$.

Besides the linear controller (Equation (15)), many different linear and non-linear feedback controls can be used to ensure convergence to zero of the tracking error. For instance, sliding mode control, high-gain control, passivity based control, model-free control, among others.

Remark 3 *An alternative method to the feedback linearization, is the exact feedforward linearization presented in [25] where the problem of type "division by zero" in the control design is easily avoided. This control method removes the need for asymptotic observers since in its design the system states information is replaced by their corresponding reference trajectories. The robustness of the exact feedforward linearization was analyzed in [27].*

4 Preliminaries on Symbolic Bézier trajectory

To create a trajectory that passes through several points, we can use approximating or interpolating approaches. The interpolating trajectory that passes through the points is prone to oscillatory effects (more unstable), while the approximating trajectory like the Bézier curve or B-Spline curve is more convenient since it only approaches defined so-called *control points* [13] and have

simple geometric interpretations. The Bézier/B-spline curve can be handled by conveniently handling the curve's control points.

The main reason in choosing the Bézier curves over the B-Splines curves, is the simplicity of their arithmetic operators presented further in this Section. Despite the nice local properties of the B-spline curve, the direct symbolic multiplication⁴ of B-splines lacks clarity and has partly known practical implementation [39].

In the following Section, we start by presenting the *Bézier curve* and its properties. Bézier curves are chosen to construct the reference trajectories because of their nice properties (smoothness, strong convex hull property, derivative property, arithmetic operations). They have their own type basis function, known as the Bernstein basis, which establishes a relationship with the so-called control polygon. A complete discussion about Bézier curves can be found in [41]. Here, some basic and key properties are recalled as a preliminary knowledge.

4.1 Definition of the Bézier curve

A Bézier curve is a parametric one that uses the Bernstein polynomials as a basis. An n th degree Bézier curve is defined by

$$f(t) = \sum_{j=0}^N c_j B_{j,N}(t), \quad 0 \leq t \leq 1 \quad (17)$$

where the c_j are the *control points* and the basis functions $B_{j,N}(t)$ are the *Bernstein polynomials* (see Figure 2). The $B_{j,N}(t)$ can be obtained explicitly by:

$$B_{j,N}(t) = \binom{N}{j} (1-t)^{N-j} t^j \text{ for } j = 0, \dots, N.$$

or by recursion with the De Casteljau formula:

$$B_{j,N}(t) = (1-t)B_{j,N-1}(t) + tB_{j-1,N-1}(t).$$

4.2 Bézier properties

For the sake of completeness, we here list some important Bézier-Bernstein properties.

Lemma 1 *Let n be a non-negative polynomial degree. The Bernstein functions have the following properties:*

1. *Partition of unity.* $\sum_{j=0}^n B_{j,N}(t) \equiv 1$

This property ensures that the relationship between the curve and its defining Bézier points is invariant under affine transformations.

⁴The multiplication operator is essential when we want to work with polynomial systems.

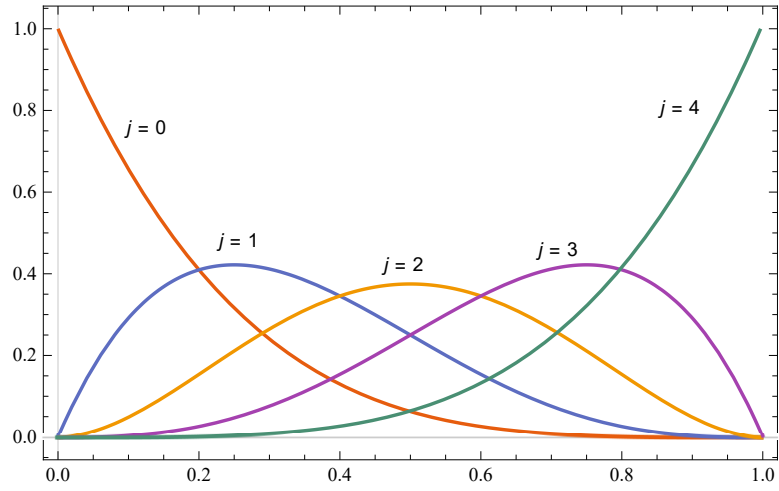


Figure 2: Bernstein Basis for degree $N = 4$.

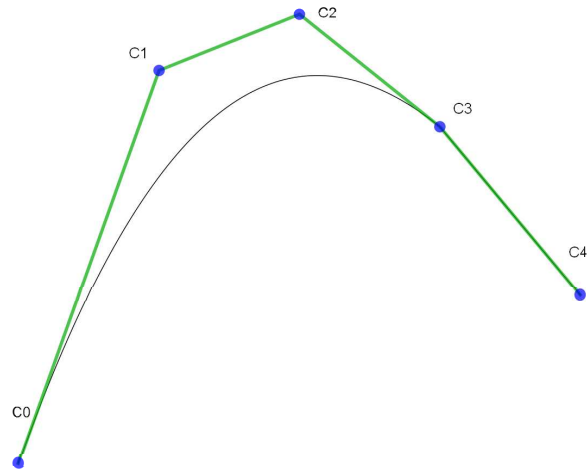


Figure 3: The convex hull property for Bézier curve ($N = 4$) with control points $c_j (j = 0, \dots, 4)$.

2. *Positivity.* If $t \in [0, 1]$ then $B_{j,N}(t) > 0$.
It guarantees that the curve segment lies completely within the convex hull of the control points (see Figure 3).
3. *Tangent property.* For the start and end point, this guarantees $f(0) = c_0$ and $f(1) = c_N$ but the curve never passes through the intermediate control points.
4. *Smoothness.* $B_{j,N}(t)$ is $N - 1$ times continuously differentiable. Hence, increasing degree increases regularity.

4.3 Quantitative envelopes for the Bézier curve

Working with the Bézier curve control points in place of the curve itself allows a simpler explicit representation. However, since our framework is not based on the Bézier curve itself, we are interested in the localisation of the Bézier curve with respect to its control points, *i.e.* the control polygon. In this part, we review a result on *sharp quantitative bounds* between the Bézier curve and its control polygon [40, 32]. For instance, in the case of a quadrotor (discussed in Section 7.2), once we have selected the control points for the reference trajectory, these envelopes describe the exact localisation of the quadrotor trajectory and its distance from the obstacles. These quantitative envelopes may be of particular interest when avoiding corners of obstacles which traditionally in the literature [42] are modelled as additional constraints or introducing safety margin around the obstacle.

We start by giving the definition for the control polygon.

Definition 1 (*Control polygon for Bézier curves (see [40])*). Let $f = \sum_{j=0}^N c_j B_{j,N}(t)$ be a scalar-valued Bézier curve. The control polygon $\Gamma_f = \sum_{j=0}^N c_j H_j(t)$ of f is a piecewise linear function connecting the points with coordinates (t_j^*, c_j) for $j = 0, \dots, N$ where the first components $t_j^* = \frac{j}{N}$ are the Greville abscissae. The hat functions H_j are piecewise linear functions defined as:

$$H_j(t) = \begin{cases} \frac{t - t_{j-1}^*}{t_j^* - t_{j-1}^*} & t \in [t_{j-1}^*, t_j^*] \\ \frac{t_{j+1}^* - t}{t_{j+1}^* - t_j^*} & t \in [t_j^*, t_{j+1}^*] \\ 0 & \text{otherwise.} \end{cases}$$

An important detail is the *maximal distance* between a Bézier segment and its control polygon. For that purpose, we recall a result from [40], where sharp quantitative bounds of control polygon distance to the Bézier curve are given.

Theorem 1 (*See [40], Theorem 3.1*) Let $f = \sum_{j=0}^N c_j B_{j,N}$ be a scalar Bézier curve and let Γ_f be its control polygon. Then the maximal distance from f to its control polygon is bounded as:

$$\|f - \Gamma_f\|_{\infty, [0,1]} \leq \mu_\infty(N) \|\Delta_2 c\|_\infty = D_{\max} \quad (18)$$

where the constant $\mu_\infty(N) = \frac{\lfloor N/2 \rfloor \lceil N/2 \rceil}{2N}$ ⁵ only depends on the degree N and the second difference of the control points $\|\Delta_2 c\|_\infty := \max_{0 \leq j < N} |\Delta_2 c_j|$.

The j^{th} second difference of the control point sequence c_j for $j = 0, \dots, N$ is given by:

$$\Delta_2 c_j = c_{j-1} - 2c_j + c_{j+1}.$$

Based on this maximal distance, *Bézier curve's envelopes* are defined as two piecewise linear functions:

- the *lower envelope* $\underline{\Gamma}_f = \sum_{j=0}^N \underline{e}_j H_j = \sum_{j=0}^N (c_j - D_{\max}) H_j$ and,
- the *upper envelope* $\bar{\Gamma}_f = \sum_{j=0}^N \bar{e}_j H_j = \sum_{j=0}^N (c_j + D_{\max}) H_j$

such that $\underline{\Gamma}_f \leq f \leq \bar{\Gamma}_f$.

The envelopes are improved by taking $\underline{e}_0 = \bar{e}_0 = c_0$ and $\underline{e}_N = \bar{e}_N = c_N$ and then *clipped* with the standard Min-Max bounds ⁶. The Min-Max bounds yield rectangular envelopes that are defined as

Definition 2 (*Min-Max Bounding box* (see [41])). Let $f = \sum_{j=0}^N c_j B_{j,N}$ be a Bézier curve. As a consequence of the convex-hull property, a min-max bounding box is defined for the Bézier curve f as:

$$\min_{0 \leq j < N} c_j \leq \sum_{j=0}^N c_j B_{j,N} \leq \max_{0 \leq j < N} c_j.$$

Remark 4 As we notice, the maximal distance between a Bézier segment and its control polygon is bounded in terms of the second difference of the control point sequence and a constant that depends only on the degree of the polynomial. Thus, by elevating the degree of the Bézier control polygon, i.e. the subdivision (without modifying the Bézier curve), we can arbitrary reduce the distance between the curve and its control polygon.

4.4 Symbolic Bézier operations

In this section, we present the Bézier operators needed to find the Bézier control points of the states and the inputs. Let the two polynomials $f(t)$ (of degree m) and $g(t)$ (of degree n) with *control points* f_j and g_j be defined as follows:

$$f(t) = \sum_{j=0}^m f_j B_{j,m}(t), \quad 0 \leq t \leq 1$$

$$g(t) = \sum_{j=0}^n g_j B_{j,n}(t), \quad 0 \leq t \leq 1$$

⁵Note that the notation $\lceil x \rceil$ means the ceiling of x , i.e. the smallest integer greater than or equal to x , and the notation $\lfloor x \rfloor$ means the floor of x , i.e. the largest integer less than or equal to x .

⁶Unfortunately the simple Min-Max bounds define very large envelopes when applied solely.

We now show how to determine the control points for the degree elevation and for the arithmetic operations (the sum, difference, and product of these polynomials). For further information on Bézier operations, see [14]. Some illustrations of the geometrical significance of these operations are included in the Appendix A.

Degree elevation: To increase the degree from n to $n + r$ and the number of control points from $n + 1$ to $n + r + 1$ without changing the shape, the new control points b_j of the $(n + r)$ th Bézier curve are given by:

$$b_j = \sum_{i=\max(0, j-r)}^{\min(n, j)} \frac{\binom{n}{i} \binom{r}{j-i}}{\binom{n+r}{j}} g_i \quad j = 0, 1, \dots, n + r \quad (19)$$

The latter constitutes the so-called *augmented control polygon*. The new control points are obtained as convex combinations of the original control points. This is an important operation exploited in addition/subtraction of two control polygons of different lengths and in approaching the curve to a new control polygon by refining the original one.

Addition and subtraction: If $m = n$ we simply add or subtract the coefficients

$$f(t) \pm g(t) = \sum_{j=0}^m (f_j \pm g_j) B_{j,m}(t) \quad (20)$$

If $m > n$, we need to first elevate the degree of $g(t)$ $m - n$ times using (19) and then add or subtract the coefficients.

Multiplication: Multiplication of two polynomials of degree m and n yields a degree $m + n$ polynomial

$$f(t)g(t) = \sum_{j=0}^{m+n} \underbrace{\left(\sum_{i=\max(0, j-n)}^{\min(m, j)} \frac{\binom{m}{i} \binom{n}{j-i}}{\binom{m+n}{j}} f_i g_{j-i} \right)}_{\text{Control points of the product}} B_{j, m+n}(t) \quad (21)$$

4.5 Bézier time derivatives

We give the derivative property of the Bézier curve in Proposition 1 which is crucial in establishing the constrained trajectory procedure.

Lemma 2 (see [33]) *The derivative of the j th Bernstein function of degree $n \geq 1$ is given by*

$$DB_{j,N}(t) = N (B_{j-1, N-1}(t) - B_{j, N-1}(t)) \text{ for } j = 0, \dots, N. \quad (22)$$

for any real number t and where $B_{-1, N-1} = B_{N, N-1} = 0$.

Proposition 1 *If the flat output or the reference trajectory y is a Bézier curve, its derivative is still a Bézier curve and we have an explicit expression for its control points.*

Proof 1 *Let $y^{(q)}(t)$ denote the q th derivative of the flat output $y(t)$. We use the fixed time interval $T = t_f - t_0$ to define the time as $t = T\tau$, $0 \leq \tau \leq 1$. We can obtain $y^{(q)}(\tau)$ by computing the q th derivatives of the Bernstein functions.*

$$y^{(q)}(\tau) = \frac{1}{T^q} \sum_{j=0}^N c_j B_{j,N}^{(q)}(\tau) \quad (23)$$

Letting $c_j^{(0)} = c_j$, we write

$$y(\tau) = y^{(0)}(\tau) = \sum_{j=0}^N c_j^{(0)} B_{j,N}(\tau) \quad (24)$$

Then,

$$y^{(q)}(\tau) = \sum_{j=0}^{N-q} c_j^{(q)} B_{j,N-q}(\tau) \quad (25)$$

with derivative control points such that

$$c_j^{(q)} = \begin{cases} c_j, & q = 0 \\ \frac{(N-q+1)}{T^q} (c_{j+1}^{(q-1)} - c_j^{(q-1)}), & q > 0. \end{cases} \quad (26)$$

We can deduce the explicit expressions for all lower order derivatives up to order $N - 1$. This means that if the reference trajectory $y_r(t)$ is a Bézier curve of degree $N > q$ (q is the derivation order of the flat output y), by differentiating it, all states and inputs are given in straightforward Bézier form.

Example 1 *Through a simple example of a double integrator, we want to represent the link between the time interval and the time derivatives. For a changing position y , its time derivative \dot{y} is its velocity, and its second derivative with respect to time \ddot{y} , is its acceleration. Even higher derivatives are sometimes also used: the third derivative of position with respect to time is known as the jerk.*

We here want to show the effect of the fixed time period T on the velocity, acceleration, etc. We remark the connection between the time scaling parameter appearing in the trajectory parameterization. We have a simple double integrator defined as:

$$\ddot{y} = u \quad (27)$$

As a reference trajectory, we choose a Bézier curve $y = \sum_{i=0}^N a_i B_{i,N}$ of order $N = 4$. Due to the Bézier derivative property, we can explicitly provide the link

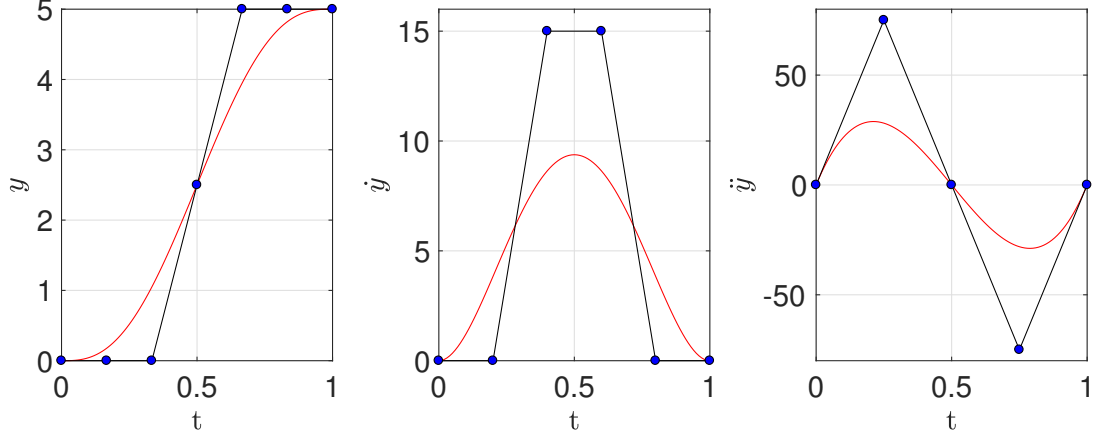


Figure 4: The time derivatives when $T = 1$

between the time interval T and control points of the Bézier curve's derivatives.

$$\dot{y} = \sum_{i=0}^{N-1} a_i^{(1)} B_{i,N-1} \quad (28a)$$

$$\ddot{y} = \sum_{i=0}^{N-2} a_i^{(2)} B_{i,N-2} \quad (28b)$$

where $a_i^{(1)}$ and $a_i^{(2)}$ are the control points of the first and the second derivative of the B-spline curve respectively. We have the expressions of the $a_i^{(1)}$ and $a_i^{(2)}$ in terms of the a_i . This fact allow us to survey when the desired reference trajectory will respect the input constraints i.e. $a_i^{(2)} = f_1(a_i^{(1)}) = f_2(a_i)$. That means that if $\forall a_i^{(2)} < K$ then $u < K$.

Proposition 2 If we take a Bézier curve as reference trajectory $y_r(t) = \sum_{j=0}^N c_j B_{j,N}(t)$ for a flat system such that the input is a polynomial function of the flat output and its derivatives, then the open loop input is also a Bézier curve $u_r = B(y_r, \dots, y_r^{(q)}) = \sum_{i=0}^m U_i B_{i,m}(t)$.

Remark 5 We should take a Bézier curve of degree $N > q$ to avoid introducing discontinuities in the control input.

Example 2 In the case of a chain of integrators $u_r(t) = y_r^{(q)}(t)$ by imposing for all $K_l \leq c_j^{(q)} \leq K_h$, we ensure an input constraint $K_l \leq u_r(t) \leq K_h$.

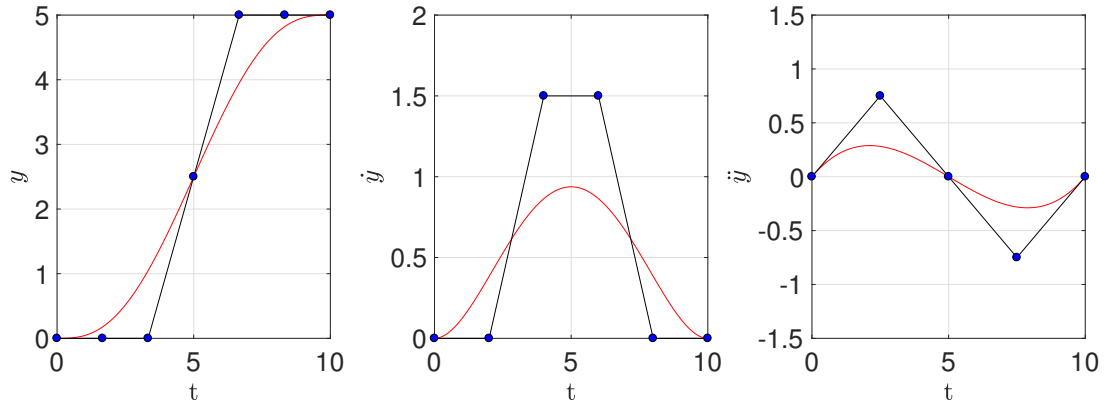


Figure 5: The time derivatives when $T = 10$

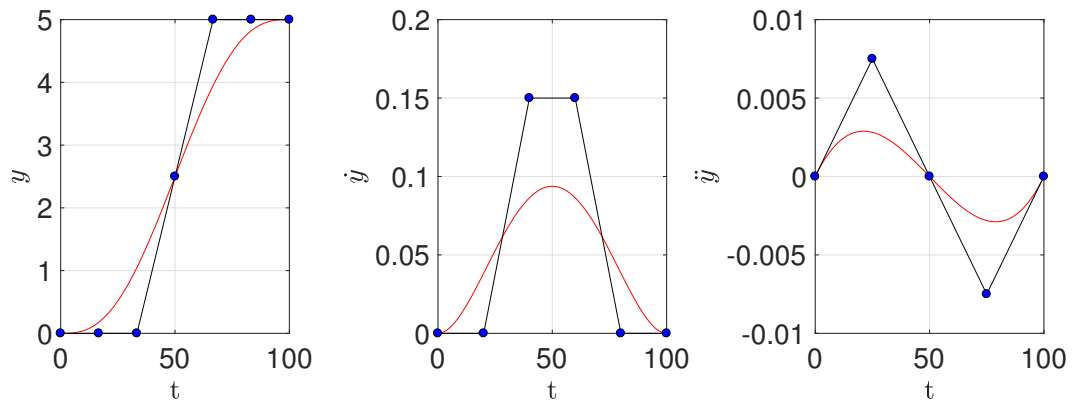


Figure 6: The time derivatives when $T = 100$

5 Constrained feedforward trajectory procedure

We aim to find a feasible Bézier trajectory (or a set of feasible trajectories, and then make a suitable choice) $\mathbf{y}_r(t)$ between the initial conditions $\mathbf{y}_r(t_0) = \mathbf{y}_{\text{initial}}$ and the final conditions $\mathbf{y}_r(t_f) = \mathbf{y}_{\text{final}}$. We here show the procedure to obtain the *Bézier control points* for the constrained nominal trajectories $(\mathbf{y}_r, \mathbf{x}_r, \mathbf{u}_r)$.

Given a *differentially flat system* $\dot{\mathbf{x}} = f(\mathbf{x}, \mathbf{u})$, the reference design procedure can be summarized as:

1. Assign to each flat output (trajectory) y_i a *symbolic Bézier curve* $y_i(t) = \sum_{j=0}^N \alpha_j B_{j,N}(t)$ of a suitable degree $N > q$ (q is the time derivatives of the flat output) and where $\boldsymbol{\alpha} = (\alpha_0, \dots, \alpha_N) \in \mathbb{R}^{N+1}$ are its control points.
2. Compute the needed derivatives of the flat outputs using Equation (25).
3. Use the Bézier operations to produce the system model relationships (11)-(12), and to find the *state reference Bézier curve* $\mathbf{x}_r(t) = \sum_{i=0}^m X_i B_{i,m}(t)$ and *input reference Bézier curve* $\mathbf{u}_r(t) = \sum_{j=0}^m U_j B_{j,m}(t)$ respectively, such that $(X_i, U_j) = r_k(\alpha_0, \dots, \alpha_N), k = 0, \dots, m + n + 2$ are functions of the *output control points*.
4. If needed, calculate the corresponding *augmented control polygons* by elevating the degree of the original control polygons in order to be closer to the Bézier trajectory.
5. Specify the initial conditions, final conditions, or intermediate conditions on the flat output or on any derivative of the flat output that represent a direct equality constraint on the Bézier control points. Each flat output trajectory has its control points fixed as follows:

$$\alpha_0^{(i)} = y^{(i)}(t_0), \quad (29a)$$

$$\alpha_N^{(i)} = y^{(i)}(t_f), \text{ for } i = 0, \dots, q, \quad (29b)$$

$$\alpha_j \in [\underline{\alpha}_j, \bar{\alpha}_j] \text{ for } j = 1, \dots, N - 1, \quad (29c)$$

where $\underline{\alpha}_j, \bar{\alpha}_j \in \mathbb{R}$ are the limits of the j^{th} control point. By using the Bézier properties, we will construct a set of constraints by means of its control points. We have a special case for the parallellotope where the first and last control point are fixed $\underline{\alpha}_0 = \bar{\alpha}_0 = y(t_0)$ and $\underline{\alpha}_N = \bar{\alpha}_N = y(t_f)$ respectively.

6. We consider a constrained method based on the Bézier control points since the control point polygon captures important geometric properties of the

Bézier curve shape. The conditions on the output Bézier control points α_j , the state Bézier control points X_i and the input control points U_j result in a semi-algebraic set (system of polynomial equations and/or inequalities) defined as:

$$\mathcal{J}(r, \mathbb{A}) = \{\alpha \in \mathbb{A} \mid r_k(\alpha) *_{\leq} 0, k \in \{1, \dots, l\}, *_{\leq} \in \{<, \leq, >, \geq, =, \neq\}\} \quad (30)$$

Depending on the studied system, the output constraints can be defined as in equation (13), or remain as $\mathbb{A} = \mathbb{R}^{N+1}$.

7. Find the regions of the *control points* α_j , $j = 1, \dots, N - 1$, solving the system of equality/inequalities (30) by using an appropriate method. We present two kind of possible methods in Section 6.

6 Feasible control points regions

Once we transform all the system trajectories through the symbolic Bézier flat output, the problem is formulated as a system of functions (equations and inequalities) with Bézier control points as parameters (see equation (30)). Consequently the following question raises:

Question 2 *How to find the regions in the space of the parameters (Bézier control points) where the system of functions remains valid i.e. the constrained set of feasible feed-forwarding trajectories?*

This section has the purpose to answer the latter question by reviewing two methods from *semialgebraic geometry*⁷:

In *the first method*, we formulate the regions for the reference trajectory control points search as a *Quantifier Elimination (QE)* problem. The QE is a powerful procedure to compute an *equivalent* quantifier-free formula for a given first-order formula over the reals [48, 11]. Here we briefly introduce the QE method.

Let $f_i(X, U) \in \mathbb{Q}[X, U]$, $i = 1, \dots, l$ be polynomials with rational coefficients where:

- $X = (x_1, \dots, x_n) \in \mathbb{R}^n$ is a vector of quantified variables
- $U = (u_1, \dots, u_m) \in \mathbb{R}^m$ is a vector of unquantified (free) variables.

The *quantifier-free* Boolean formula $\varphi(X, U)$ is a combined expression of polynomial equations ($f_i(X, U) = 0$), inequalities ($f_i(X, U) \leq 0$), inequations ($f_i(X, U) \neq 0$) and strict inequalities ($f_i(X, U) > 0$) that employs the logic

⁷The theory that studies the real-number solutions to algebraic inequalities with-real number coefficients, and mappings between them, is called semialgebraic geometry.

operators \wedge (and), \vee (or), \Rightarrow (implies) or \Leftrightarrow (equivalence).
A prenex or *first-order formula* is defined as follows:

$$G(X, U) = (Q_1 x_1) \dots (Q_n x_n) [\varphi(X, U)]$$

where Q_i is one of the quantifiers \forall (for all) and \exists (there exists). Following the Tarski Seidenberg theorem (see [11]), for every prenex formula $G(X, U)$ there exists an equivalent quantifier-free formula $\psi(U)$ defined by the free variables.

The goal of the QE procedure is to compute an equivalent quantifier free formula $\psi(U)$ for a given first-order formula. It finds the feasible regions of free variables U represented as semialgebraic set where $G(X, U)$ is true. If the set U is non-empty, there exists a point $u \in \mathbb{R}^m$ which simultaneously satisfies all of the equations/inequalities. Such a point is called a feasible point and the set U is then called feasible. If the set U is empty, it is called unfeasible. In the case when $m = 0$, *i.e.* when all variables are quantified, the QE procedure decides whether the given formula is true or false (decision problem). For instance,

- given a first order formula $\forall x [x^2 + bx + c > 0]$, the QE algorithm gives the equivalent quantifier free formula $b - 4c < 0$;
- given a first order formula $\exists x [ax^2 + bx + c = 0]$, the QE algorithm gives the equivalent quantifier free formula $(a \neq 0 \wedge b^2 - 4ac \geq 0) \vee (a = 0 \wedge b \neq 0) \vee (a = 0 \wedge b = 0 \wedge c = 0)$.

As we can notice, the quantifier free formulas represent the semi-algebraic sets (the conditions) for the unquantified free variables verifying the first order formula is *true*. Moreover, given an input formula without quantifiers, the QE algorithm produces a *simplified formula*. For instance (for more examples, see [5]),

- given an input formula $(ab \leq 0) \wedge (a + b = 0) \wedge (b^2 + a^2 > 0) \vee (a^2 = -b^2)$, the QE algorithm gives the equivalent simplified formula $a + b = 0$.

On the other hand, given an input formula without unquantified free variables (usually called closed formula) is either *true* or *false*.

The symbolic computation of the *Cylindrical Algebraic Decomposition* (CAD) introduced by Collins [10] is the best currently known QE algorithm for solving real algebraic constraints (in particular parametric and *non-convex* case) (see [46]). This method gives us *an exact solution*, a simplified formula describing the semi-algebraic set.

The QE methods, particularly the CAD, have already been used in various aspects of control theory (see [43, 1] and the references therein): robust control design, finding the feasible regions of a PID controller, the Hurwitz and Schur stability regions, reachability analysis of nonlinear systems, trajectory generation [30].

Remark 6 (*On the complexity*) Unfortunately the above method rapidly becomes slow due to its double exponential complexity [34]. Its efficiency strongly depends on the number and on the complexity of the variables (control points) used for a given problem. The computational complexity of the CAD is double exponential i.e. bounded by $(sd)^{2^{\mathcal{O}(n)}}$ for a finite set of s polynomials in n variables, of degree d . There are more computationally efficient QE methods than the CAD, like the Critical Point Method [4] (it has single exponential complexity in n the number of variables) and the cylindrical algebraic sub-decompositions [52] but to the author knowledge there are no available implementations.

For more complex systems, the exact or symbolic methods are too computationally expensive. There exist methods that are numerical rather than exact.

As a second alternative method, we review one such method based on approximation of the exact set with more reasonable computational cost. The second method known as the Polynomial Superlevel Set (PSS) method, based on the paper [12] instead of giving us exact solutions tries to approximate the set of solutions by minimizing the L^1 norm of the polynomial. It can deal with more complex problems.

6.1 Cylindrical Algebraic Decomposition

In this section, we give a simple introduction to the Cylindrical Algebraic Decomposition.

Input of CAD: As an input of the CAD algorithm, we define a set of polynomial equations and/or inequations in n unknown symbolic variables (in our case, the control points) defined over real interval domains.

Definition of the CAD: The idea is to develop a sequence of projections that drops the dimension of the semi-algebraic set by one each time. Given a set S of polynomials in R^n , a *cylindrical algebraic decomposition* is a decomposition of R^n into finitely many connected semialgebraic sets called *cells*, on which each polynomial has constant sign, either $+$, $-$ or 0 . To be cylindrical, this decomposition must satisfy the following condition: If $1 \leq k < n$ and π is the projection from R^n onto R^{n-k} consisting in removing the k last coordinates, then for every pair of cells c and d , one has either $\pi(c) = \pi(d)$ or $\pi(c) \cap \pi(d) = \emptyset$. This implies that the images by π of the cells define a cylindrical decomposition of R^{n-k} .

Output of CAD: As an output of this symbolic method, we obtain the total algebraic expressions that represent *an equivalent simpler form* of our system. Ideally, we would like to obtain a parametrization of all the control points regions as a closed form solution. Finally, in the case where closed forms are computable for the solution of a problem, one advantage is to be able to overcome

any optimization algorithm to solve the problem for a set of given parameters (numerical values), since only an evaluation of the closed form is then necessary.

The execution runtime and memory requirements of this method depend of the dimension of the problem to be solved because of the computational complexity. For the implementation part, we will use its *Mathematica* implementation⁸ (developed by Adam Strzebonski). Other implementations of CAD are QEPCAD, Redlog, SyNRAC, Maple.

Example 3 *From [28], we present an example in which we want to find the regions of the parameters $(a, b) \in \mathbb{R}^2$ where the following formula is true, not only answering if the formula is true or not. Having as input*

$$F = \left\{ (a, b) \in \mathbb{R}^2 : f_1(a, b) = \sqrt{a^2 - b^2} + \sqrt{ab - b^2} - a > 0, \quad f_2(a, b) = 0 < b < a \right\}$$

the corresponding CAD output is given by

$$\left\{ a > 0 \wedge b < \frac{4}{5}a \right\}$$

As we notice, given a system of equations and inequalities formed by the control points relationship as an input, the CAD returns a simpler system that is equivalent over the reals.

6.2 Approximations of Semialgebraic Sets

Here we present a method based on the paper [12] that tries to approximate the set of solutions. Given a set

$$\mathcal{K} = \{x \in \mathbb{R}^n : g_i(x) \geq 0, i = 1, 2, \dots, m\}$$

which is compact, with non-empty interior and described by given real multi-variable polynomials $g_i(x)$ and a compact set $\mathcal{B} \supset \mathcal{K}$, we aim at determining a so-called *polynomial superlevel set* (PSS)

$$U(p) = \{x \in \mathcal{B} : p(x) \geq 1\}$$

The set \mathcal{B} is assumed to be an n -dimensional hyperrectangle. The PSS can capture the main characteristics of \mathcal{K} (it can be non convex and non connected) while having at the same time a simpler description than the original set. It consists in finding a polynomial p of degree d whose 1-superlevel set $\{x \mid p(x) \geq 1\}$ contains a semialgebraic set \mathcal{B} and has minimum volume. Assuming that one is given a simple set \mathcal{B} containing \mathcal{K} and over which the integrals of polynomials can be efficiently computed, this method involves searching for a polynomial p

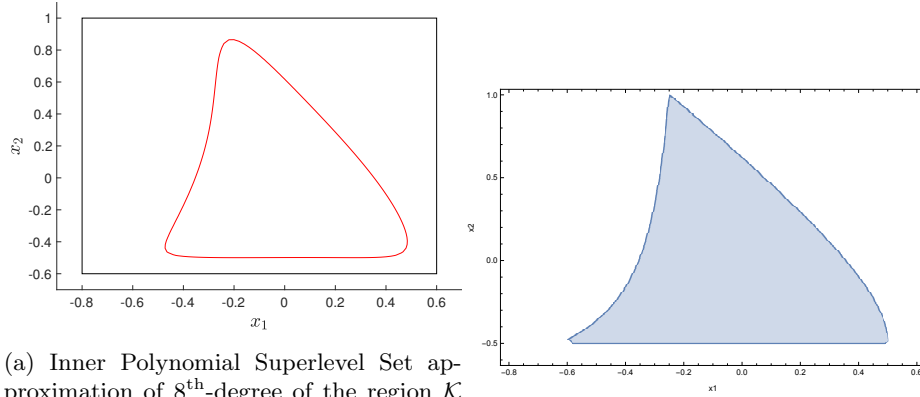
⁸see <https://reference.wolfram.com/language/ref/CylindricalDecomposition.html>

of degree d which minimizes $\int_{\mathcal{B}} p(x) dx$ while respecting the constraints $p(x) \geq 1$ on \mathcal{K} and $p(x) \geq 0$ on \mathcal{B} . Note that the objective is linear in the coefficients of p and that these last two nonnegativity conditions can be made computationally tractable by using the *sum of squares relaxation*. The complexity of the approximation depends on the degree d . The advantage of such a formulation lies in the fact that when the *degree* of the polynomial p increases, the objective value of the problem converges to the true volume of the set \mathcal{K} .

Example 4 *To better review the latter method, we illustrate it with an example for a two dimensional set given in [12]. In order to compare the two presented methods, we also give its CAD solution. Having the following non-convex semi-algebraic set:*

$$\mathcal{K} = x \in \mathbb{R}^2 : \begin{cases} f_1(x) = 1 + 2x_2 \geq 0, \\ f_1(x) = 2 - 4x_1 - 3x_2 \geq 0, \\ f_1(x) = 10 - 28x_1 - 5x_2 - 24x_1x_2 - 18x_2^2 \geq 0, \\ f_1(x) = 1 - x_2 - 8x_1^2 - 2x_1x_2 - x_2^2 - 8x_1^2x_2 - 6x_1x_2^2 \geq 0 \end{cases}$$

with a bounding box $\mathcal{B} = [-0.8, 0.6] \times [-0.6, 1.0]$, and setting $d = 8$, the degree of the polynomial $p(x)$. The algorithm yields the feasible region represented in Figure 7a.



(a) Inner Polynomial Superlevel Set approximation of 8th-degree of the region \mathcal{K} (the inner surface of the red line). The black rectangle represents the bounding box. (b) The region found by the CAD algorithm (the inner surface of the blue line).

Figure 7: The feasible regions by the two methods

For the same set, even without specifying a particular box, the CAD algo-

irithm finds the following explicit solution:

$$\begin{aligned}
& \left(x_1 = -\frac{5}{8} \wedge x_2 = -\frac{1}{2} \right) \\
& \vee \left(-\frac{5}{8} < x_1 < -\frac{1}{6} \wedge -\frac{1}{2} \leq x_2 \leq \frac{-8x_1^2 - 2x_1 - 1}{2(6x_1 + 1)} - \frac{1}{2} \sqrt{\frac{64x_1^4 - 160x_1^3 - 12x_1^2 + 28x_1 + 5}{(6x_1 + 1)^2}} \right) \\
& \vee \left(x_1 = -\frac{1}{6} \wedge -\frac{1}{2} \leq x_2 \leq \frac{7}{8} \right) \\
& \vee \left(-\frac{1}{6} < x_1 < \frac{1}{2} \wedge -\frac{1}{2} \leq x_2 \leq \frac{-8x_1^2 - 2x_1 - 1}{2(6x_1 + 1)} + \frac{1}{2} \sqrt{\frac{64x_1^4 - 160x_1^3 - 12x_1^2 + 28x_1 + 5}{(6x_1 + 1)^2}} \right) \\
& \vee \left(x_1 = \frac{1}{2} \wedge x_2 = -\frac{1}{2} \right)
\end{aligned}$$

As we can observe, the PSS method (Figure 7a) gives us a good approximation of the feasible region, almost the same as the exact one obtained by the CAD algorithm (Figure 7b). However, in some cases, we observed that the PSS method may have some sensibilities when its bounding box is not well defined.

7 Applications

7.1 Longitudinal dynamics of a vehicle

The constraints are essentials in the design of vehicle longitudinal control which aims to ensure the passenger comfort, safety and fuel/energy reduction. The longitudinal control can be designed for a highway scenario or a city scenario. In the first scenario, the vehicle velocity keeps a constant form where the main objective is the vehicle inter-distance while the second one, deals with frequent stops and accelerations, the so-called Stop-and-Go scenario [50]. The inter-distance dynamics can be represented as an single integrator driven by the difference between the leader vehicle velocity V_l and the follower vehicle velocity V_x , i.e., $\dot{d} = V_l - V_x$.

In this example, suppose we want to follow the leader vehicle, and stay within a fixed distance from it (measuring the distance through a camera/radar system). Additionally, suppose we enter a desired destination through a GPS system, and suppose our GPS map contains all the speed information limits. Our goal is the follower longitudinal speed V_x to follow a reference speed $V_{xr}(t) \in [0, \min(V_l, V_{\max})]$, $V_{\max} \in \mathbb{R} > 0$ given by the minimum between the leader vehicle speed and the speed limit.

The longitudinal dynamics of a follower vehicle is given by the following model:

$$M\dot{V}_x(t) = \frac{u(t)}{r} - C_a V_x^2(t) \quad (31)$$

where V_x is the longitudinal speed of the vehicle, u is the motor torque, taken as *control input* and the physical constants: M the vehicle's mass, r the mean

wheel radius, and C_a the aerodynamic coefficient.

The model is differentially flat, with V_x as a flat output. An open loop control yielding the tracking of the reference trajectory V_{xr} by V_x , assuming the model to be perfect, is

$$u_r(t) = r \left(M \dot{V}_{xr}(t) + C_a V_{xr}^2(t) \right) \quad (32)$$

If we desire an open-loop trajectory $u_r \in C^0$, then for the flat output, we should assign a Bézier curve of degree $d > 1$. We take V_{xr} as reference trajectory, a Bézier curve of degree 4 *i.e.* C^4 -function.

$$V_{xr}(t) = \sum_{i=0}^4 a_i B_{i,4}(t),$$

$$V_{xr}(t_0) = V_i, \quad V_{xr}(t_f) = V_f$$

where the a_i 's are the control points and the $B_{i,4}$ the Bernstein polynomials. Using the Bézier curve properties, we can find the control points of the open-loop control u_r in terms of the a_i 's by the following steps:

1. First, we find the control points $a_i^{(1)}$ for \dot{V}_{xr} by using the Equation (26):

$$\dot{V}_{xr} = \sum_{i=0}^3 a_i^{(1)} B_{i,3}(t)$$

2. We obtain the term V_{xr}^2 by

$$V_{xr}^2 = \sum_{i=0}^4 a_i B_{i,4}(t) \sum_{i=0}^4 a_i B_{i,4}(t) = \sum_{i=0}^8 p_i B_{i,8}(t)$$

which is a Bézier curve of degree 8 and where the control points p_i are computed by the multiplication operation (see Equation (21)).

3. We elevate the degree of the first term up to 8 by using the Equation (19) and then, we find the sum of the latter with the Bézier curve for V_{xr}^2 . We end up with u_r as a Bézier curve of degree 8 with nine control points U_i :

$$u_r(t) = r M \dot{V}_{xr} + r C_a V_{xr}^2 = r M \sum_{i=0}^3 a_i B_{i,3}(t) + r C_a \left(\sum_{i=0}^4 a_i B_{i,4}(t) \right)^2 = \sum_{i=0}^8 U_i B_{i,8}(t)$$

with $U_i = r_k(a_0, \dots, a_4)$.

7.1.1 Symbolic input constraints

We want the input control points U_i to be

$$U_{\min} < U_i < U_{\max} \quad i = 0, \dots, 8 \quad (33)$$

where $U_{\min} = 0$ is the lower input constraint and $U_{\max} = 10$ is the high input constraint. By limiting the control input, we indirectly constraint the fuel consumption. The initial and final trajectory control points are defined as $V_x(t_0) = a_0 = 0$ and $V_x(t_1) = a_4 = 1$ respectively.

The constraint (33) directly corresponds to the semi-algebraic set: The constraint (33) corresponds to the *semi-algebraic set i.e.* the following system of nonlinear inequalities:

$$\begin{cases} 0 < U_0 = 4a_1 < 10 \\ 0 < U_1 = a_1 + \frac{3a_2}{2} < 10 \\ 0 < U_2 = \frac{4a_1^2}{7} - \frac{5a_1}{7} + \frac{12a_2}{7} + \frac{3a_3}{7} < 10 \\ 0 < U_3 = \frac{15a_2}{14} - \frac{10a_1}{7} + a_3 + \frac{6a_1a_2}{7} + \frac{1}{14} < 10 \\ 0 < U_4 = \frac{18a_2^2}{35} - \frac{10a_1}{7} + \frac{10a_3}{7} + \frac{16a_1a_3}{35} + \frac{2}{7} < 10 \\ 0 < U_5 = \frac{10a_3}{7} - \frac{15a_2}{14} - \frac{6a_1}{7} + \frac{6a_2a_3}{7} + \frac{5}{7} < 10 \\ 0 < U_6 = \frac{4a_3^2}{7} + \frac{5a_3}{7} - \frac{3a_1}{7} - \frac{9a_2}{7} + \frac{10}{7} < 10 \\ 0 < U_7 = \frac{5}{2} - \frac{3a_2}{2} < 10 \\ 0 < U_8 = 5 - 4a_3 < 10 \end{cases} \quad (34)$$

In order to solve symbolically the system of inequalities *i.e.* to find the regions of the intermediate control points a_i , we use the Mathematica function *CylindricalDecomposition*. The complete symbolic solution with three intermediate control points (a_1, a_2, a_3) is too long to be included. Since the latter is too long to be included, we illustrate the symbolic solution in the case of two intermediate control points (a_1, a_2) :

$$\begin{aligned} & (0 < a_1 \leq 0.115563 \wedge -a_1 < a_2 < 1.33333) \\ & \vee (0.115563 < a_1 \leq 0.376808 \wedge 0.142857(-3a_1^2 + 2a_1 - 1) < a_2 < 1.33333) \\ & \vee \left(0.376808 < a_1 \leq 1.52983 \wedge \frac{4a_1 - 2}{3a_1 + 4} < a_2 < 1.33333 \right) \\ & \vee (1.52983 < a_1 < 2 \wedge 0.33333\sqrt{15a_1 - 17} - 0.33333 < a_2 < 1.33333) \end{aligned}$$

The latter solution describing the feasible set of trajectories can be used to make a choice for the Bézier control points: "First choose a_1 in the interval $(0, 0.115563]$ and then you may choose a_2 bigger than the chosen $-a_1$ and smaller than 1.33333. Or otherwise choose a_1 in the interval $(0.115563, 0.376808]$ and, then choose a_2 such that $0.142857(-3a_1^2 + 2a_1 - 1) < a_2 < 1.33333$, etc."

In Figure 8, we illustrate the feasible regions for the three intermediate control points (a_1, a_2, a_3) by using the Mathematica function *RegionPlot3D*. We can observe how the flat outputs influences the control input *i.e.* which part of the reference trajectory influences which part of the control input. For instance in (34), we observe that the second control point a_1 influences more than a_2 and a_3 the beginning of the control input (the control points U_0, U_1, U_2). The

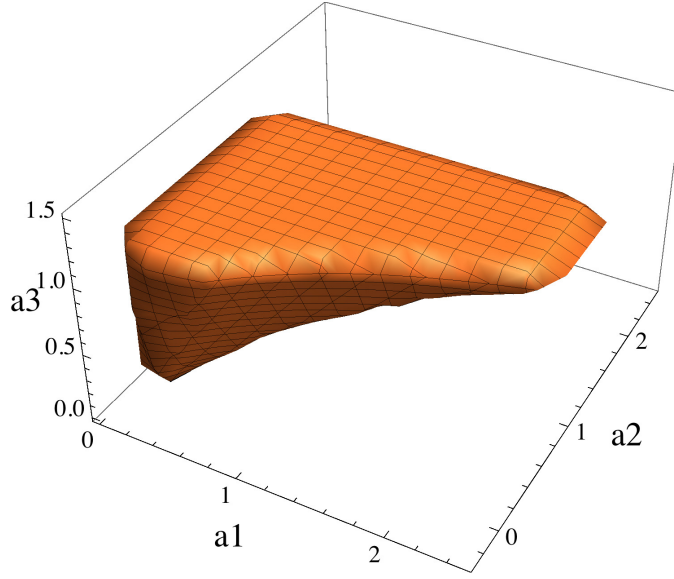


Figure 8: Feasible region for the control points of V_{xr} when $U_{\min} = 0$ and $U_{\max} = 10$.

previous inequalities can be used as a prior study to the sensibility of the control inputs with respect to the flat outputs.

It should be stressed that the goal here is quite different than the traditional one in optimisation problems. We do not search for the best trajectory according to a certain criterion under the some constraints, but we wish to obtain the set of all trajectories fulfilling the constraints; this for an end user to be able to pick one or another trajectory in the set and to switch from one to another in the same set. The picking and switching operations aim to be really fast.

7.1.2 Simulation results

The proposed control approach has been successfully tested in simulation. For the physical parameters of the vehicle, academic values are chosen to test the constraint fulfilment. For the design of the Bézier reference trajectory, we pick values for a_1, a_2 and a_3 in the constrained region. As trajectory control points for V_{xr} , we take the possible feasible choice $a_0 = 0, a_1 = 2, a_2 = 2.3, a_3 = 1.3, a_4 = 1$. Simulation results for the constrained open-loop input are shown in Figure 9.

The form of the closed-loop input is

$$u = Mr \left(\dot{V}_{xr} - \lambda(V_x - V_{xr}) \right) + rC_a V_x^2 \quad (35)$$

where $\lambda = 9$ is the proportional feedback gain chosen to make the error dynamics

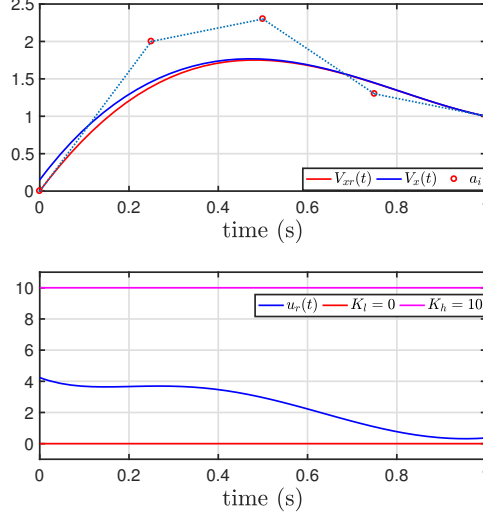


Figure 9: Open-loop input control

stable. Figure 10 shows the performance of the closed-loop control. For both schemes, the input respects the limits.

As shown in Figure 11, choosing a control point outside of the suitable region ($a_1 = 5.5$) can violate the closed-loop input limits.

7.2 Quadrotor dynamics

7.2.1 Motivation

Over the last decade, the quadrotors have been a subject of extensive research study and have been used in a wide range of industrial and commercial applications. The quadrotors have become so popular due to their agility that allows them to hover as well as takeoff and land vertically while still being able to perform *aggressive trajectories*⁹.

However, during aggressive trajectory design, it is difficult to ensure trajectory feasibility while trying to exploit the entire range of feasible motor inputs. Moreover, in many applications, their role is to fly in complex cluttered environments, hence there is a necessity of output constraints. Therefore, the constraints on the inputs and states are one of the crucial issues in the control of quadrotors.

Fortunately, with the hardware progress, today the quadrotors have speed limits of forty meters per second and more comparing to few meters per second in

⁹A trajectory is considered as an aggressive one if during its tracking, one of the quadrotor motors is close to a saturation.

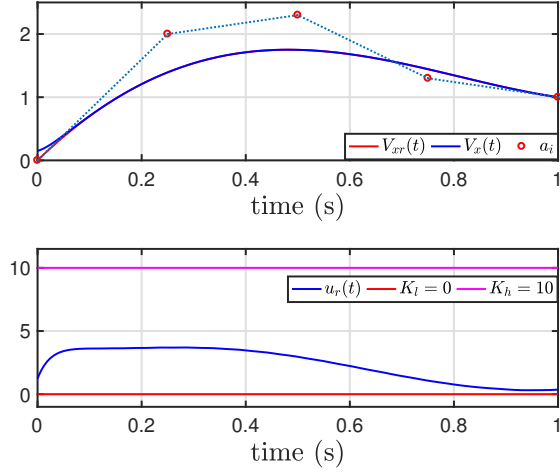


Figure 10: Closed-loop performance of trajectory tracking

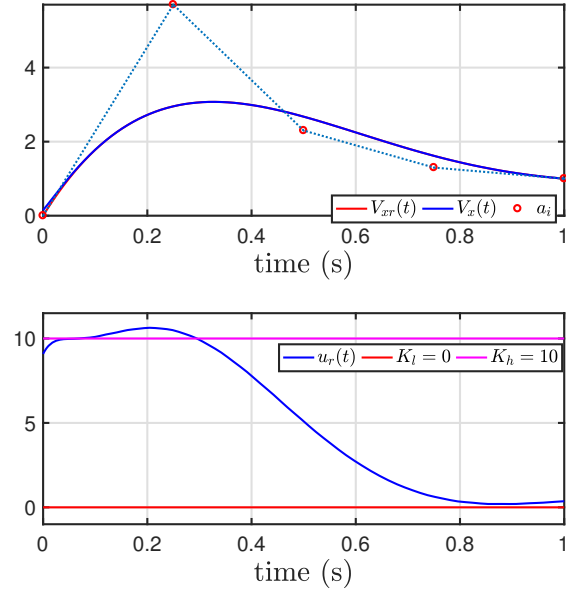


Figure 11: When control point a_1 is out of its region

the past [15]. Therefore, it is important to conceive control laws for quadrotors to a level where they can exploit their full potential especially in terms of agility.

In the famous paper [38], is proposed an algorithm that generates optimal trajectories such that they minimize cost functionals that are derived from the square of the norm of the snap (the fourth derivative of position). There is a limited research investigating the quadrotor constraints (see [6] and the papers therein) without employing an online optimisation.

The following application on quadrotor is devoted to unify the dynamics constraints or demands constraints with the environmental constraints (*e.g.* , fixed obstacles).

7.2.2 Simplified model of quadrotor

A (highly) simplified nonlinear model of quadrotor is given by the equations:

$$m\ddot{x} = \theta u_1 \quad (36a)$$

$$m\ddot{y} = -\phi u_1 \quad (36b)$$

$$m\ddot{z} = -mg + u_1 \quad (36c)$$

$$I_x\ddot{\theta} = u_2 \quad (36d)$$

$$I_y\ddot{\phi} = u_3 \quad (36e)$$

$$I_z\ddot{\psi} = u_4 \quad (36f)$$

where x , y and z are the position coordinates of the quadrotor in the world frame, and θ , ϕ and ψ are the pitch, roll and yaw rotation angles respectively. The constant m is the mass, g is the gravitation acceleration and I_x, I_y, I_z are the moments of inertia along the y, x directions respectively. The thrust u_1 is the total lift generated by the four propellers applied in the z direction, and u_2, u_3 and u_4 are the torques in θ, ϕ and ψ directions respectively. As we can notice, the quadrotor is an under-actuated system *i.e.* it has six degrees of freedom but only four inputs.

A more complete presentation of the quadrotor model can be found in the Section ??.

7.2.3 Differential flatness of the quadrotor

Here, we describe the quadrotor differential parametrization on which its offline reference trajectory planning procedure is based. The model (36) is differentially flat. Having four inputs for the quadrotor system, the flat output has four components. These are given by the vector:

$$F = (x, y, z, \psi).$$

By equation (36c), we easily obtain expression of the thrust reference u_{1r}

$$u_{1r} = m(\ddot{z}_r + g) \quad (37)$$

Then, by replacing the thrust expression in (36a)–(36b), we obtain the angles θ_r and ϕ_r given by

$$\theta_r = \frac{m\ddot{x}_r}{u_{1r}} = \frac{\ddot{x}_r}{\ddot{z}_r + g} \quad (38a)$$

$$\phi_r = \frac{-m\ddot{y}_r}{u_{1r}} = \frac{-\ddot{y}_r}{\ddot{z}_r + g} \quad (38b)$$

We then differentiate (38a), (38b) and ψ_r twice to obtain (36d)–(36f) respectively. This operation gives us u_2 , u_3 and u_4 .

$$u_{2r} = I_x \ddot{\theta}_r = \frac{I_x}{(g + \ddot{z}_r)} \left(x_r^{(4)} - 2 \frac{x_r^{(3)}(\ddot{z}_r + g) - \ddot{x}_r z_r^{(3)}}{(\ddot{z}_r + g)^2} z_r^{(3)} - \frac{\ddot{x}_r z_r^{(4)}}{\ddot{z}_r + g} \right), \quad (39)$$

$$u_{3r} = I_y \ddot{\phi}_r = \frac{I_y}{(g + \ddot{z}_r)} \left(-y_r^{(4)} + 2 \frac{y_r^{(3)}(\ddot{z}_r + g) - \ddot{y}_r z_r^{(3)}}{(\ddot{z}_r + g)^2} z_r^{(3)} + \frac{\ddot{y}_r z_r^{(4)}}{\ddot{z}_r + g} \right), \quad (40)$$

and

$$u_{4r} = I_z \ddot{\psi}_r. \quad (41)$$

A more complete model of a quadrotor and its flatness parametrization can be found in [44] and [21].

7.2.4 Constraints

Given an initial position and yaw angle and a goal position and yaw angle of the quadrotor, we want to find a set of smooth reference trajectories while respecting the dynamics constraints and the environmental constraints. Quadrotors have electric DC rotors that have limits in their rotational speeds, so input constraints are vital to avoid rotor damage. Besides the state and input constraints, to enable them to operate in constrained spaces, it is of great importance to impose output constraints.

We consider the following constraints:

1. *The thrust u_1*

We set a maximum ascent or descending acceleration of $4g$ ($g=9.8 \text{ m/s}^2$), and hence the thrust constraint is defined as:

$$0 < u_1 \leq U_1^{\max} = 4m \cdot g = 20.79 \text{ N}, \quad (42)$$

where m is the quadrotor mass which is set as 0.53 kg in the simulation. By the latter constraint, we also avoid the singularity for a zero thrust.

2. *The pitch and roll angle*

In applications, the tilt angle is usually inferior to 14 degrees (0.25 rad). We set

$$|\phi| \leq \Phi^{\max} = 0.25 \text{ rad} \quad (43)$$

$$|\theta| \leq \Theta^{\max} = 0.25 \text{ rad} \quad (44)$$

3. *The torques u_2 , u_3 et u_4*

With a maximum tilt acceleration of 48 rad/s^2 , the limits of the control inputs are:

$$|u_2|, |u_3| \leq 48I_{xx} = 0.3 \text{ N}\cdot\text{m} \quad (45)$$

$$|u_4| \leq 48I_{zz} = 0.5 \text{ N}\cdot\text{m} \quad (46)$$

where I_{xx} , I_{yy} , I_{zz} are the parameters of the moment of inertia, $I_{xx} = I_{yy} = 6.22 \times 10^{-3} \text{ kg}\cdot\text{m}^2$, $I_{zz} = 1.12 \times 10^{-2} \text{ kg}\cdot\text{m}^2$.

4. *Collision-free constraint*

To avoid obstacles, constraints on the output trajectory x, y, z should be reconsidered.

Scenario 1: In this scenario, we want to impose constraints on the thrust, and on the roll and pitch angles.

7.2.5 Constrained open-loop trajectory u_{1r}

We specialize the flat output z_r to a sigmoid between two quasi constant altitudes, a situation frequently needed in practice:

$$z_r(t) = \frac{H_f - H_i}{2} (1 + \tanh(\gamma(t - t_m))) + H_i \quad (47)$$

where H_i is the initial altitude and H_f is the final altitude of the quadrotor; γ is the slope parameter of the tanh and t_m is the time when the quadrotor is taking off (see Figure 12). The maximum value for $z_r(t)$ is the final altitude H_f (see fig. 12).

The easy numerical implementation of the derivatives of $z_r(t)$ is due to the nice recursion. Let $R = \tanh(\gamma(t - t_m))$ and $C = \frac{H_f - H_i}{2}$. The first four derivatives of $z_r(t)$ are given as:

$$\begin{aligned} \dot{z}_r &= \gamma C (1 - R^2) \\ \ddot{z}_r &= -2\gamma^2 C R (1 - R^2) \\ z_r^{(3)} &= 2\gamma^3 C (1 - R^2)(1 - 3R^2) \\ z_r^{(4)} &= -8\gamma^4 C R (3R^4 - 5R^2 + 2) \end{aligned}$$

The maximum values for its derivatives depend only on γ and C , and their

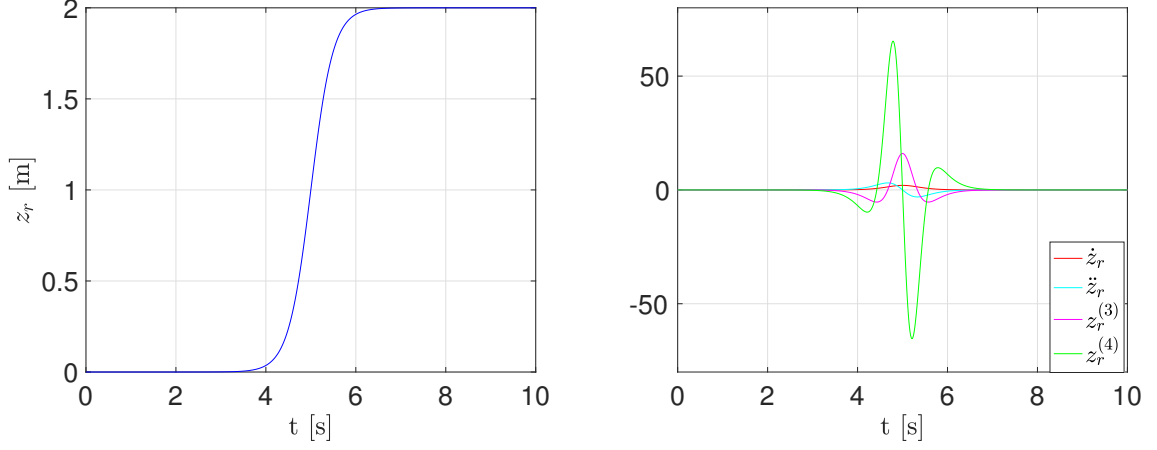


Figure 12: The reference trajectory for $z_r(t)$ (left) and its derivatives (right) with $H_i = 0\text{m}$ and $H_f = 2\text{m}$, $t_m = 5\text{s}$ and parameter $\gamma = 2$.

values can be determined. We obtain their bounds as:

$$\begin{aligned}
 H_i &\leq z_r \leq H_f, & b_1 &= 1; \\
 0 &\leq \dot{z}_r \leq b_1 \gamma C, & b_2 &= \frac{4\sqrt{3}}{9}; \\
 -b_2 \gamma^2 C &\leq \ddot{z}_r \leq b_2 \gamma^2 C, & \underline{b}_3 &= \frac{2}{3}, \quad \overline{b}_3 = 2; \\
 -\underline{b}_3 \gamma^3 C &\leq z_r^{(3)} \leq \overline{b}_3 \gamma^3 C, & b_4 &\approx 4.0849. \\
 -b_4 \gamma^4 C &\leq z_r^{(4)} \leq b_4 \gamma^4 C,
 \end{aligned}$$

Consequently, from the thrust limits (42), we have the following inequality

$$0 < m(-b_2 \gamma^2 + g) \leq u_{1r} = m(\ddot{z}_r + g) \leq m(b_2 \gamma^2 + g) < U_1^{\max}.$$

The input constraint of u_{1r} will be respected by choosing a suitable value of γ and C such that

$$\gamma^2 C < \min \left\{ \frac{1}{b_2} \left(\frac{U_1^{\max}}{m} - g \right), \frac{g}{b_2} \right\}. \quad (48)$$

Figure 13 depicts the constrained open-loop trajectory u_{1r} that is well chosen by taking $\gamma = 2$ and $H_f = 2\text{m}$. On the other hand, in Figure 14 is shown the violation of the thrust constraints when $\gamma = 7$ is chosen out of the constrained interval (48).

7.2.6 Constrained open-loop trajectories θ_r et ϕ_r

In the rest of the study, we omit the procedure for the angle ϕ_r since is the same as for the angle θ_r .

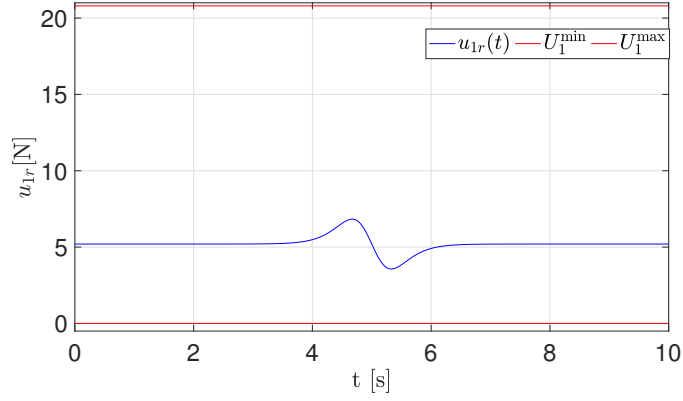


Figure 13: The reference trajectory for $u_{1r}(t)$ for a value of $\gamma = 2$ and $H_f = 2\text{m}$.

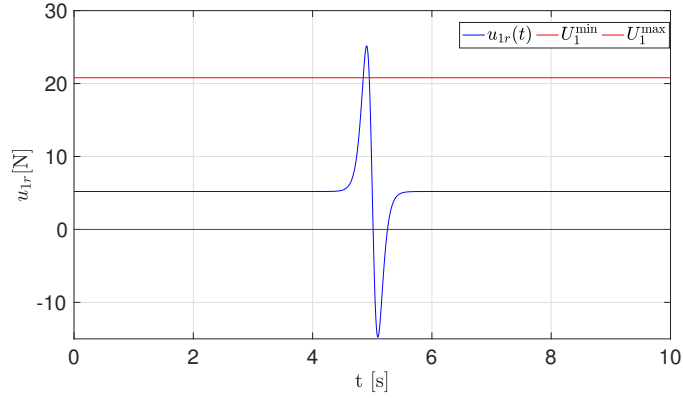


Figure 14: When the value for γ is out of the defined interval, the constraints on the open-loop trajectory $u_{1r}(t)$ are not respected. The reference trajectory for $u_{1r}(t)$ for a value of $\gamma = 7$.

1. In the first attempt, the reference trajectory x_r will be a Bézier curve of degree $d = 6$ with a predefined control polygon form as:

$$\mathbf{A}_{\mathbf{x}} = \left\{ a, a, a, \frac{a+b}{2}, b, b, b \right\}.$$

The aim of the first and the final control point repetitions is to fix the velocity and acceleration reference equilibrium points as : $\dot{x}_r(t_0) = \dot{x}_r(t_f) = 0$ and $\ddot{x}_r(t_0) = \ddot{x}_r(t_f) = 0$.

The control polygon of the velocity reference trajectory \dot{x} is :

$$\mathbf{A}_{\dot{x}} = \left\{ 0, 0, \frac{d}{T} \frac{b-a}{2}, \frac{d}{T} \frac{b-a}{2}, 0, 0 \right\}.$$

The control polygon of the acceleration reference trajectory \ddot{x} is :

$$\mathbf{A}_{\ddot{x}} = \left\{ 0, \frac{d(d-1)}{T^2} \frac{a+b}{2}, 0, -\frac{d(d-1)}{T^2} \frac{a+b}{2}, 0 \right\}.$$

The proposed form of Bézier curve provide us the explicit bounds of its second derivative \ddot{x}_r when $a = 0$ such that $\ddot{x}_r^{\min} = -\frac{144}{25} \frac{b}{T^2}$ and $\ddot{x}_r^{\max} = \frac{144}{25} \frac{b}{T^2}$.

From the Equations (43) and (38a), we get

$$\frac{-\frac{144}{25} \frac{b}{T^2}}{b_2 \gamma^2 C + g} \leq \theta_r = \frac{\ddot{x}_r}{\ddot{z}_r + g} \leq \frac{\frac{144}{25} \frac{b}{T^2}}{-b_2 \gamma^2 C + g} \quad (49)$$

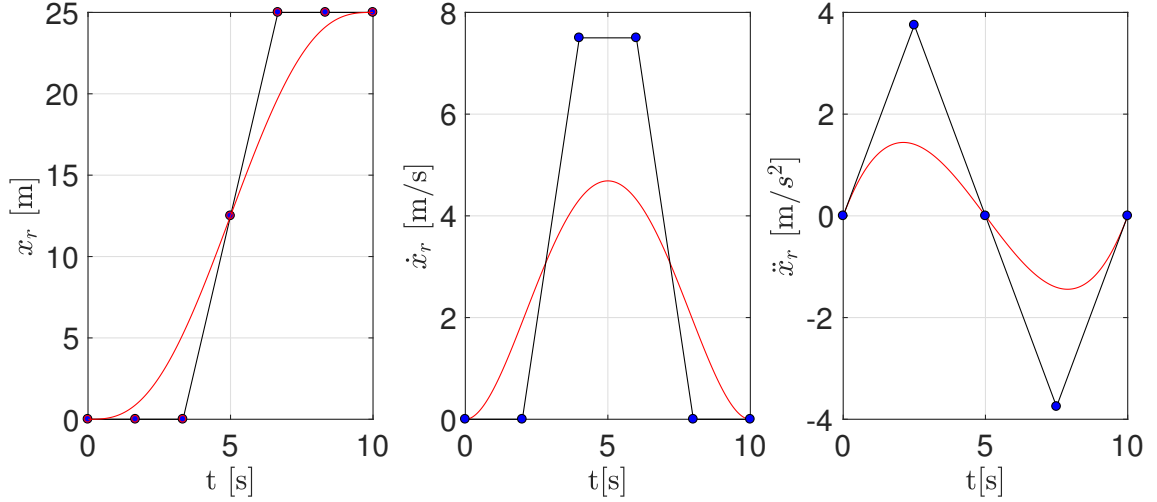


Figure 15: The Sigmoid Bézier trajectory x_r , the velocity trajectory \dot{x}_r and the acceleration trajectory \ddot{x}_r with their respective control polygons when $a = 0$ and $b = 25$.

2. In a second case, the reference trajectory x_r can be any Bézier curve. However, we need to impose the first and last controls points in order to fix the initial and final equilibrium states. For the example, we take a Bézier trajectory of degree $d = 8$ with control polygon defined as:

$$\mathbf{A}_{\mathbf{x}} = \{a, a, a, \alpha_1, \alpha_2, \alpha_3, b, b, b\}.$$

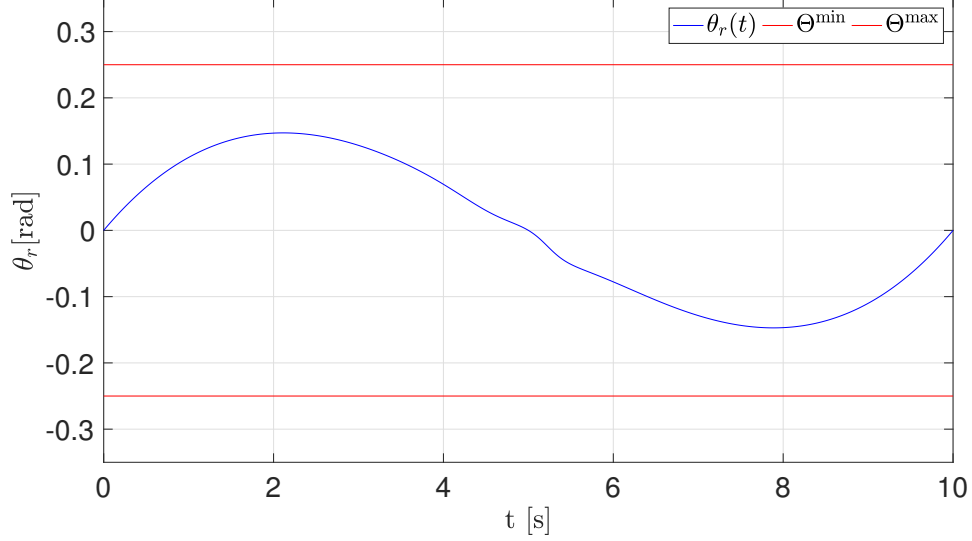


Figure 16: The open-loop trajectory $\theta_r(t)$ for Sigmoid Bézier trajectory

When $\gamma = 2$ and $H_i = 0\text{m}$, $H_f = 2\text{m}$ are fixed, the minimum and maximum values for \ddot{z}_r are also fixed. Therefore, to impose constraints on θ_r , it remains to determine \ddot{x}_r , *i.e.* the control points of x_r

$$\ddot{x}_r \leq (-b_2\gamma^2 C + g)\Theta^{\max} = X^{\max} \approx 1.682\text{m/s}^2, \quad (50)$$

$$\ddot{x}_r \geq -(b_2\gamma^2 C + g)\Theta^{\min} = X^{\min} \approx -3.222\text{m/s}^2. \quad (51)$$

The initial and final trajectory control points are defined as $x_r(t_0) = a = 0$ and $x_r(t_f) = b = 2$ respectively. Therefore, for \ddot{x}_r where $T = t_f - t_0 = 10$, we obtain the following control polygon $\mathbf{A}_{\ddot{x}} = (a_{\ddot{x}i})_{i=0}^6$:

$$\mathbf{A}_{\ddot{x}} = \left\{ 0, \frac{14\alpha_1}{25}, \frac{14\alpha_2 - 28\alpha_1}{25}, \frac{14\alpha_1 - 28\alpha_2 + 14\alpha_3}{25}, \frac{14\alpha_2 - 28\alpha_3 + 28}{25}, \frac{14\alpha_3 - 28}{25}, 0 \right\}.$$

As explained in the previous section, to reduce the distance between the control polygon and the Bézier curve, we need to elevate the degree of the control polygon $\mathbf{A}_{\ddot{x}}$. We elevate the degree of $\mathbf{A}_{\ddot{x}}$ up to 16 and we obtain a new augmented control polygon $\mathbf{A}_{\ddot{x}}^A$ by using the operation (19) (see Figure 17 (right)).

The equation (50) translates into a system of linear inequalities *i.e.* *semi-algebraic set* defined as :

$$X^{\min} < a_{\ddot{x}i}^A = f(\alpha_1, \alpha_2, \alpha_3) < X^{\max} \quad i = 0, \dots, 16. \quad (52)$$

We illustrate the feasible regions for the control points by using the Mathematica function *RegionPlot3D* (see Figure 18).

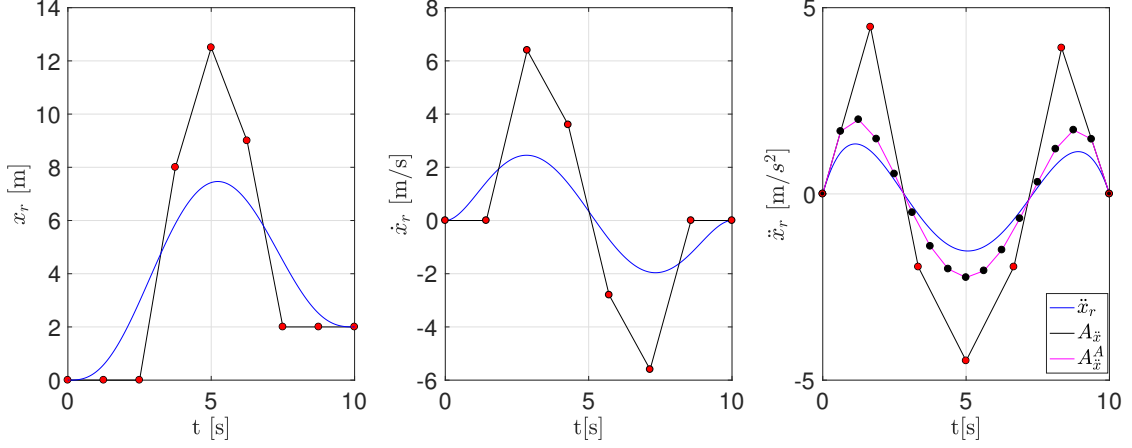


Figure 17: The Bézier curve x_r , \dot{x}_r , \ddot{x}_r (blue lines) and their respective control polygons (black linear piecewise lines) with $a = 0$, $\alpha_1 = 8$, $\alpha_2 = 12.5$, $\alpha_3 = 9$ and $b = 2$. The augmented control polygon for \ddot{x}_2 is represented by the magenta line.

Scenario 2: In this scenario, we discuss the output constraints.

7.2.7 Constrained open-loop trajectories x_r and y_r

Here we discuss the scenario when the quadrotor has already been take off by an initial Bézier curve that fulfils the previous input/state constraints and avoids the known static obstacles. Then, suddenly appear new obstacle in the quadrotor environment. To decide, whether the quadrotor should change its trajectory or continue to follow the initial trajectory, we use the quantitative envelopes of the Bézier trajectory presented in Section 4.3 to verify if its envelope region overlaps with the regions of the new obstacle.

We construct the quantitative envelopes for x_r and y_r using Section 4.3. We find the maximal distance of the Bézier curve w.r.t. to the chosen control polygon. We choose as intermediate control points for x_r and y_r ($\alpha_1 = 8$; $\alpha_2 = 12.5$; $\alpha_3 = 9$ and $\beta_1 = 4$; $\beta_2 = 2.5$; $\beta_3 = 2$ respectively). The bounded region of the chosen reference trajectories x_r and y_r are depicts in Figure 21.

In particular, the figure 20 demonstrates the benefit of the bounded trajectory region. We can precisely determine the distance between the quadrotor pathway and the obstacles.

Scenario 3: In this scenario, we discuss the input constraints u_2 and u_3 when the quadrotor is in *hover mode* i.e. moving in a horizontal plane.

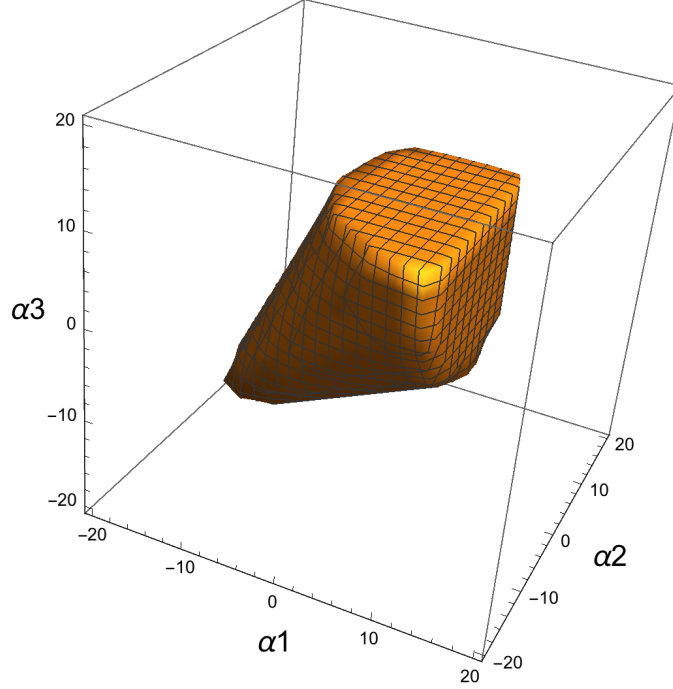


Figure 18: Feasible region for the intermediate control points of $x_r(t)$ while fulfilling the constraints on the roll angle.

7.2.8 Constrained open-loop trajectories u_2 and u_3

By the previous constraints on θ_r and u_{1r} , we implicitly constrain the torque input u_{2r} . A more general case can also be treated if we assume that when the quadrotor reaches the desired altitude, it moves in a horizontal plane. In that case by having slow dynamics for $z_r(t)$ such that $\ddot{z}_r \approx 0$, we therefore have:

$$u_{2r} = C_x x_r^{(4)} \quad (53a)$$

$$u_{3r} = C_y y_r^{(4)} \quad (53b)$$

where $C_x = \frac{I_x}{g}$ and $C_y = -\frac{I_y}{g}$ are constants. The latter forms a system of linear inequalities of the control points of x_r and y_r .

7.2.9 Constrained open-loop control for u_{4r}

For u_{4r} , we have a simple double integrator as:

$$u_{4r} = I_z \ddot{\psi}_r \quad (54)$$

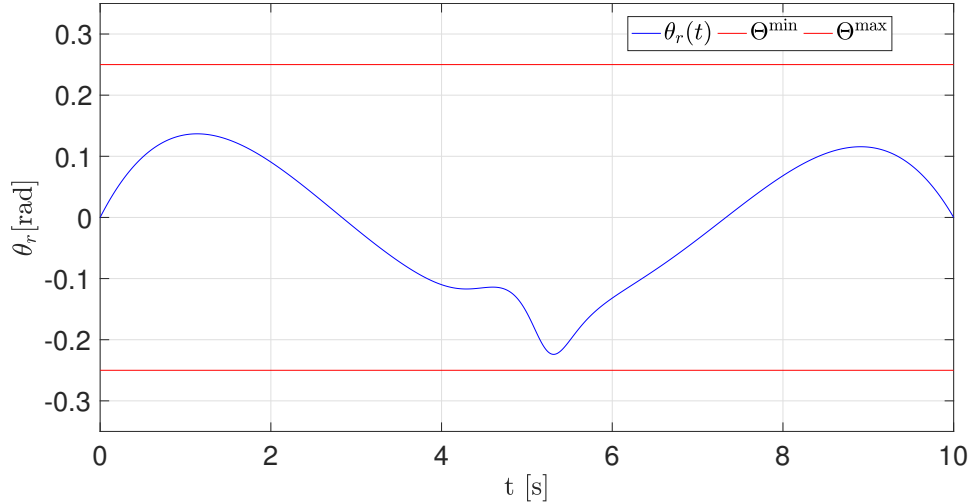


Figure 19: The constraints on the open-loop trajectory $\theta_r(t)$ are respected.

To find the regions for control points a_{ψ_i} , we proceed in the same way as in the previous Section 7.2.6.

Remark 7 *Our constrained trajectory reference study provides a set of feasible reference trajectories. Using the simplified models in the trajectory planning helps us to find the reference trajectory conform to the system dynamics constraints. On the other hand, these models can not serve as a basis for the feedback law design since it will increase the uncertainties and the mismatch with the system. For that purpose, in Chapter 4, we present the non-linear tracking of the aggressive reference trajectories by using a model-free controller.*

8 Closing remarks

We have presented a control design for non-linear flat systems handling input/state constraints through the reference trajectory design.

The state/input constraints are translated into a *system of inequalities and equalities* where the variables are the Bézier control points. This enables the input/state/output constraints to be considered into the trajectory design in a unified fashion. This allows us to develop a compact methodology to deal both with control limitations and space constraints as those arising in obstacle avoidance problems.

The core value of this work lies in two important advantages:

- The low complexity of the controller; fast real-time algorithms.

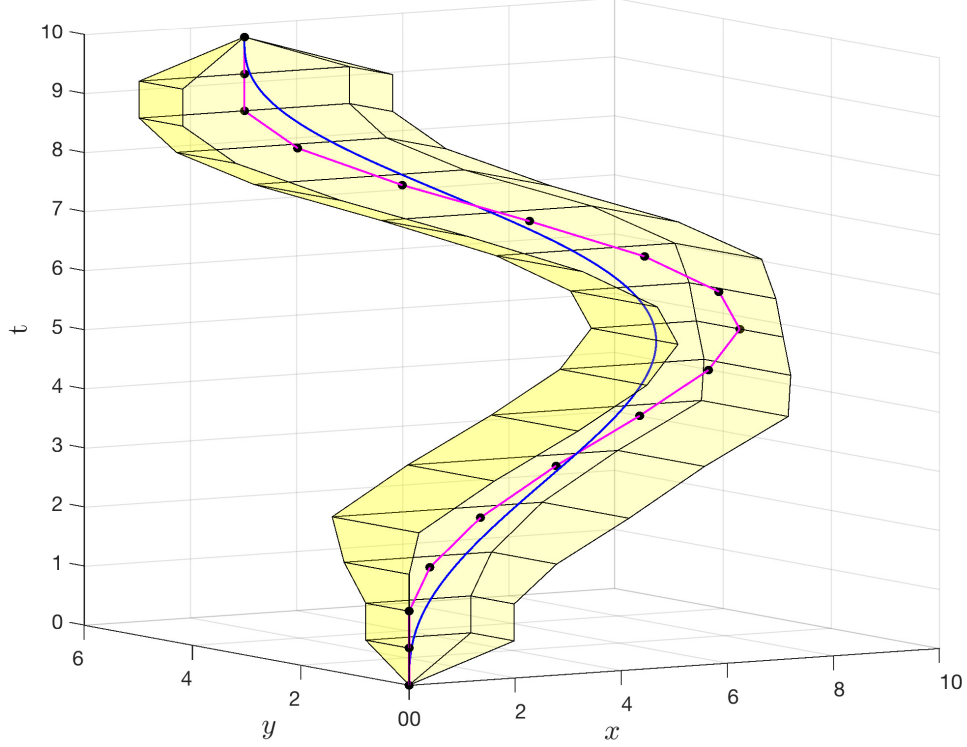


Figure 20: The constrained reference trajectories $x_r(t)$ and $y_r(t)$ and their quantitative bounded region w.r.t. to the chosen Bézier control polygon.

- The choice *i.e.* the user can select the desired feasible trajectory. The sub-optimality may be seen as a drawback.

In the context of trajectory design, we find a successful simpler or approximated semi-algebraic set defined off-line. The closed form solution of the CAD establishes an explicit relationship between the desired constraints and the trajectory parameters. This gives us a rapid insight into how the reference trajectory influences the system behaviour and the constraints fulfillment. Therefore, this method may serve as sensitivity analysis that reflects how the change in the reference trajectory influences the input reference trajectory. Also, for fault-tolerant systems, in spirit of the papers [35, 49, 9, 8], this approach may be useful for the control reconfiguration when an actuator *fault* occurs.

Our algorithm can deal with asymmetric constraints that may be useful in many situations e.g., for a vehicle where acceleration is created by a motor, while deceleration is achieved through the use of a mechanical brake. Increasing tracking errors and environment changes are signs that a re-planning of the reference trajectory is needed. Having the symbolic form of the exact solution,

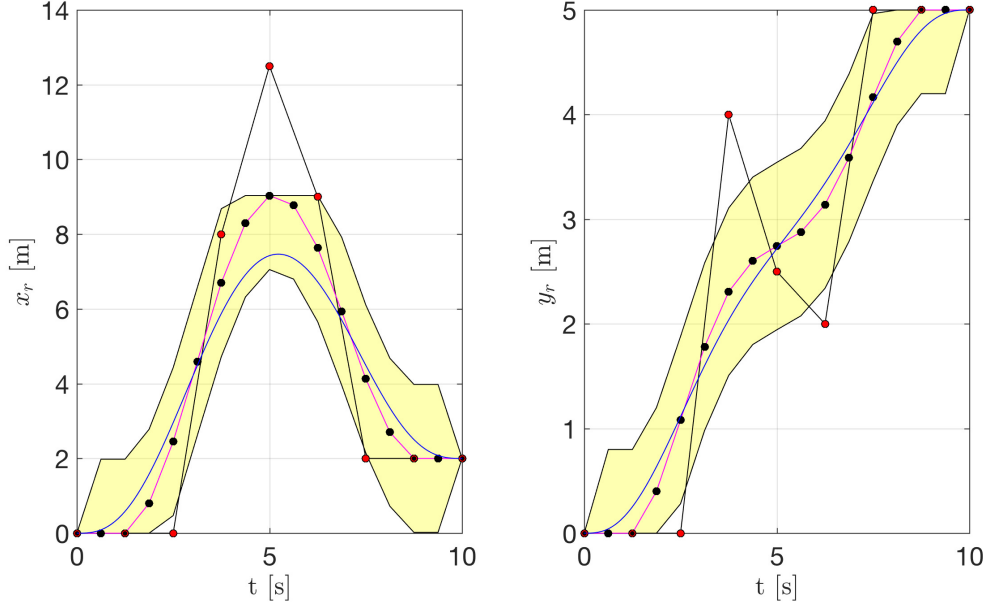


Figure 21: The quantitative envelopes for the reference trajectories $x_r(t)$ and $y_r(t)$ (the yellow highlighted regions). The augmented control polygons for $x_r(t)$ and $y_r(t)$ (magenta line). For the simulation, the intermediate control points for x_r and y_r are $\alpha_1 = 8; \alpha_2 = 12.5; \alpha_3 = 9$ and $\beta_1 = 4; \beta_2 = 2.5; \beta_3 = 2$ respectively.

allows us a quick re-evaluation over a new range of output constraints, or with a new set of numerical values for the symbolic variables. In such case, the replanning initial conditions are equivalent to the system current state.

A Geometrical signification of the Bezier operations

Here we present the geometrical signification of the degree elevation of the Bezier trajectory $y(t)$ (Figure 22), the addition (Figure 23) and the multiplication (Figure 24) of two Bézier trajectories.

B Trajectory Continuity

In the context of feedforwarding trajectories, the "degree of continuity" or the smoothness of the reference trajectory (or curve) is one of the most important

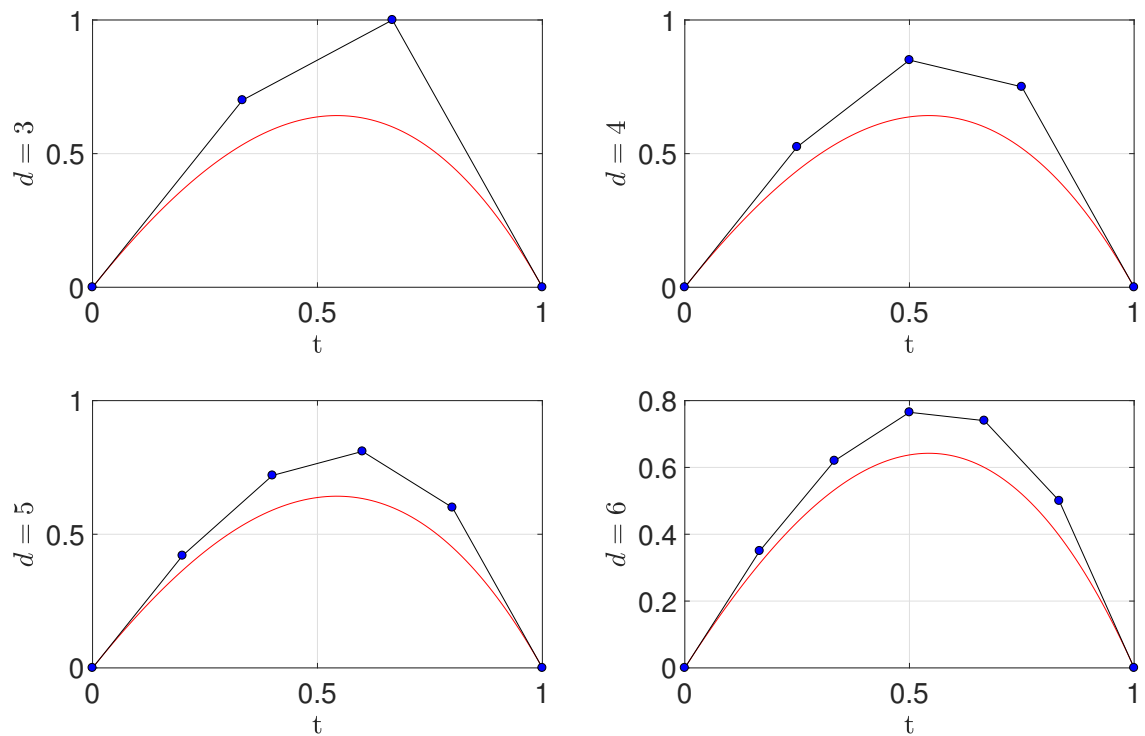


Figure 22: Degree Elevation of Bézier curve.

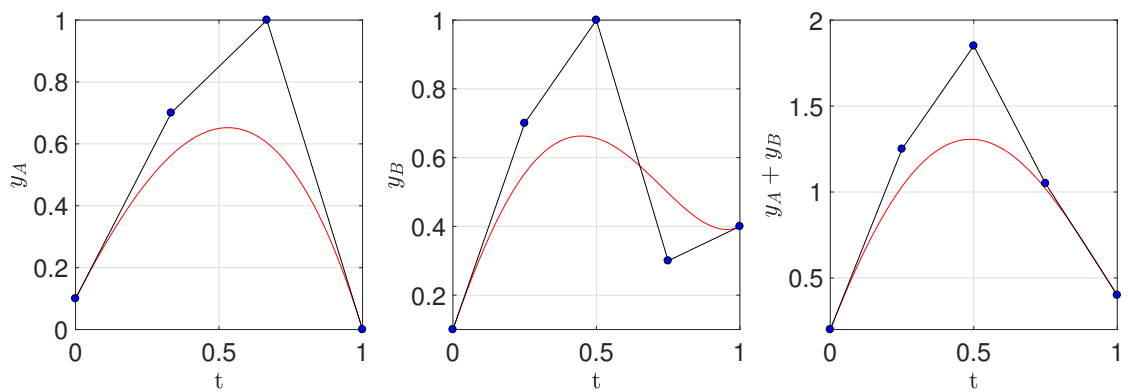


Figure 23: Addition of two Bézier curves.

factors. The smoothness of a trajectory is measured by the number of its con-

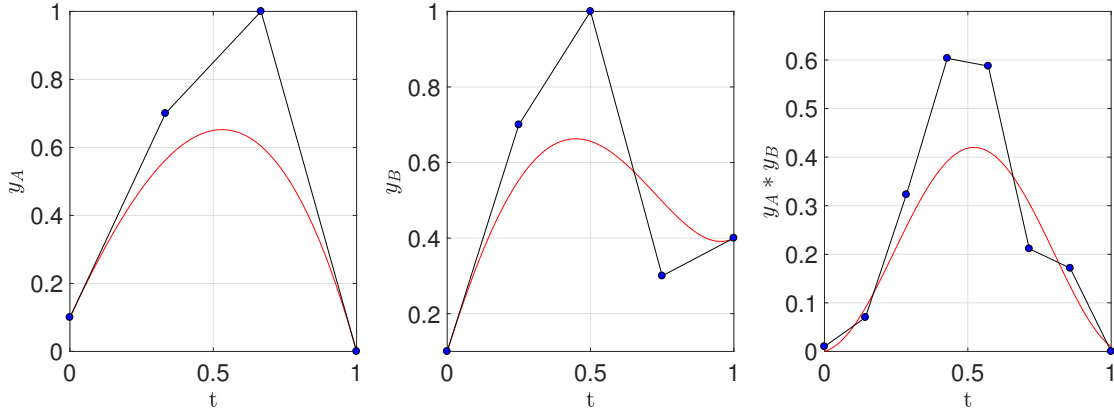


Figure 24: Multiplication of two Bézier curves.

tinuous derivatives. We here give some definitions on the trajectory continuity when it is represented by a parametric curve [3].

Parametric continuity A parametric curve $y(t)$ is n -th degree continuous in parameter t , if its n -th derivative $\frac{d^n y(t)}{dt^n}$ is continuous. It is then also called C^n continuous.

The various order of parametric continuity of a curve can be denoted as follows:

- C^0 curve *i.e.* the curve is continuous.
- C^1 curve *i.e.* first derivative of the curve is continuous. For instance, the velocity is continuous.
- C^2 curve *i.e.* first and second derivatives of the curve are continuous. (The acceleration is continuous)
- C^3 curve *i.e.* first, second and third derivatives of the curve are continuous. (the jerk is continuous)
- C^n curve *i.e.* first through n th derivatives of the curve are continuous.

Example 5 Lets take a linear curve for the joint position of a robot, as:

$$p(t) = p^i + \frac{p^f - p^i}{T_{tt}} t$$

where p^i is the initial position, p^f is the final position and T_{tt} is the time interval. We obtain for the velocity and the acceleration the following curves:

- for the velocity: $v(t) = \dot{p} = \frac{p^f - p^i}{T_{tt}}$

- for the acceleration $a(t) = \ddot{p} = \begin{cases} \infty, & t = 0, T_{tt} \\ 0, & 0 < t < T_{tt} \end{cases}$

In this example, we can observe infinite accelerations at endpoints and discontinuous velocity when two trajectory segments are connected.

References

- [1] Hirokazu Anai. Effective quantifier elimination for industrial applications. In *ISSAC*, pages 18–19, 2014.
- [2] Martin Bak. *Control of Systems with Constraints*. PhD thesis, 2000.
- [3] Brian A. Barsky and Tony D. DeRose. Geometric Continuity of Parametric Curves: Constructions of Geometrically Continuous Splines. *IEEE Computer Graphics and Applications*, 10(1):60–68, 1990.
- [4] Saugata Basu. Algorithms in real algebraic geometry: a survey. *arXiv preprint arXiv:1409.1534*, 2014.
- [5] Christopher W Brown. An overview of QEPCAD B: a tool for real quantifier elimination and formula simplification. *Journal of Japan Society for Symbolic and Algebraic Computation*, 10(1):13–22, 2003.
- [6] Ning Cao and Alan F. Lynch. Inner-Outer Loop Control for Quadrotor UAVs with Input and State Constraints. *IEEE Transactions on Control Systems Technology*, 24(5):1797–1804, 2016.
- [7] Garcia Carlos E., Prett David M., and Morari Manfred. Model Predictive Control : Theory and Practice a Survey. *Automatica*, 25(3):335–338, 1989.
- [8] Abbas Chamseddine, Youmin Zhang, Camille Alain Rabbath, Cedric Join, and Didier Theilliol. Flatness-based trajectory planning/replanning for a quadrotor unmanned aerial vehicle. *IEEE Transactions on Aerospace and Electronic Systems*, 48(4):2832–2847, 2012.
- [9] Abbas Chamseddine, Youmin Zhang, Camille Alain Rabbath, and Didier Theilliol. Trajectory Planning and Replanning Strategies Applied to a Quadrotor Unmanned Aerial Vehicle. *Journal of Guidance, Control, and Dynamics*, 35(5):1667–1671, 2012.
- [10] George E Collins. Quantifier elimination for real closed fields by cylindrical algebraic decomposition. In *Automata Theory and Formal Languages 2nd GI Conference Kaiserslautern, May 20–23, 1975*, pages 134–183. Springer, 1975.
- [11] Michel Coste. *An introduction to semialgebraic geometry*. Université de Rennes, 2002.

- [12] Fabrizio Dabbene, Didier Henrion, and Constantino M. Lagoa. Simple approximations of semialgebraic sets and their applications to control. *Automatica*, 78:110–118, 2017.
- [13] Carl de Boor. *A Practical Guide to Splines*, volume 27. Springer, New York, 2001.
- [14] Rida T Farouki and V. T. Rajan. Algorithms for polynomials in Bernstein form. *Computer Aided Geometric Design*, 5(1):1–26, 1988.
- [15] Matthias Fassler. *Quadrotor Control for Accurate Agile Flight*. PhD thesis, University of Zurich, 2018.
- [16] Timm Faulwasser, Veit Hagenmeyer, and Rolf Findeisen. Optimal exact path-following for constrained differentially flat systems. *IFAC Proceedings Volumes (IFAC-PapersOnline)*, 18(PART 1):9875–9880, 2011.
- [17] Timm Faulwasser, Veit Hagenmeyer, and Rolf Findeisen. Constrained reachability and trajectory generation for flat systems. *Automatica*, 50(4):1151–1159, 2014.
- [18] Michel Fliess. Generalized controller canonical form for linear and nonlinear dynamics. *IEEE Transactions on Automatic Control*, 35(9):994–1001, 1990.
- [19] Michel Fliess, Jean Lévine, Philippe Martin, and Pierre Rouchon. A lie-bäcklund approach to equivalence and flatness of nonlinear systems. *IEEE Transactions on Automatic Control*, 44(5):922–937, 1999.
- [20] Michel Fliess, Jean Lévine, Phillipe Martin, and Pierre Rouchon. Flatness and defect of non-linear systems: introductory theory and examples. *International Journal of Control*, 61(6):1327–1361, 1995.
- [21] Melvin E. Flores and Mark B. Milam. Trajectory generation for differentially flat systems via NURBS basis functions with obstacle avoidance. *Proceedings of the American Control Conference*, 2006:5769–5775, 2006.
- [22] Alessandro Gasparetto and Vanni Zanutto. A technique for time-jerk optimal planning of robot trajectories. *Robotics and Computer-Integrated Manufacturing*, 24(3):415–426, 2008.
- [23] Knut Graichen and Michael Zeitz. Feedforward Control Design for Finite-Time Transition Problems of Nonlinear Systems With Input and Output Constraints. *IEEE Transactions on Automatic Control*, 53(5):485–488, 2008.
- [24] Veit Hagenmeyer. Robust nonlinear tracking control based on differential flatness. *at-Automatisierungstechnik Methoden und Anwendungen der Steuerungs-, Regelungs-und Informationstechnik*, 50(12/2002):615, 2002.

- [25] Veit Hagenmeyer and Emmanuel Delaleau. Exact feedforward linearization based on differential flatness. *International Journal of Control*, 76(6):537–556, 2003.
- [26] Veit Hagenmeyer and Emmanuel Delaleau. Continuous-time non-linear flatness-based predictive control: an exact feedforward linearisation setting with an induction drive example. *International Journal of Control*, 81(10):1645–1663, 2008.
- [27] Veit Hagenmeyer and Emmanuel Delaleau. Robustness analysis with respect to exogenous perturbations for flatness-based exact feedforward linearization. *IEEE Transactions on Automatic Control*, 55(3):727–731, 2010.
- [28] Manuel Kauers. How to use cylindrical algebraic decomposition. *Seminaire Lotharingien*, 65(2011):1–16, 2011.
- [29] Steven M LaValle. *Planning algorithms*. Cambridge university press, 2006.
- [30] Stephen R Lindemann and Steven M Lavalle. Computing Smooth Feedback Plans Over Cylindrical Algebraic Decompositions. In *Robotics: Science and Systems*, Philadelphia, USA, 2006.
- [31] W. Van Loock, Goele Pipeleers, and Jan Swevers. B-spline parameterized optimal motion trajectories for robotic systems with guaranteed constraint satisfaction. *Mechanical Sciences*, 6(2):163–171, 2015.
- [32] David Lutterkort. *Envelopes of Nonlinear Geometry*. PhD thesis, Purdue University, 1999.
- [33] Tom Lyche and Knut Morken. *Spline Methods*. 2002.
- [34] Victor Magron, Didier Henrion, and Jean-Bernard Lasserre. Semidefinite approximations of projections and polynomial images of semialgebraic sets. *SIAM Journal on Optimization*, 25(4):2143–2164, 2015.
- [35] Philipp Mai, Cédric Join, and Johan Reger. Flatness-based fault tolerant control of a nonlinear MIMO system using algebraic derivative estimation To cite this version :. In *3rd IFAC Symposium on System, Structure and Control*, 2007.
- [36] Philippe Martin, Pierre Rouchon, and Richard M. Murray. *Flat systems, equivalence and trajectory generation*. 3rd cycle. edition, 2006.
- [37] David Q. Mayne, J. B. Rawlings, C. V. Rao, and P. O.M. Scokaert. Constrained model predictive control: Stability and optimality. *Automatica*, 36(6):789–814, 2000.
- [38] Daniel Mellinger and Vijay Kumar. Minimum snap trajectory generation and control for quadrotors. *Proceedings - IEEE International Conference on Robotics and Automation*, pages 2520–2525, 2011.

- [39] Knut Mørken. Some identities for products and degree raising of splines. *Constructive Approximation*, 7(1):195–208, 1991.
- [40] David Nairn, Jörg Peters, and David Lutterkort. Sharp , quantitative bounds on the distance between a polynomial piece and its Bézier control polygon. *Computer Aided Geometric Design*, 16:613–631, 1999.
- [41] Hartmut Prautzsch, Wolfgang Boehm, and Marco Paluszny. *Bézier and B-spline techniques*. Springer Science & Business Media, 2002.
- [42] Mohammadreza Radmanesh and Manish Kumar. Flight formation of UAVs in presence of moving obstacles using fast-dynamic mixed integer linear programming. *Aerospace Science and Technology*, 50(December):149–160, 2016.
- [43] Stefan Ratschan. Applications of Quantified Constraint Solving over the Reals Bibliography. *ArXiv*, pages 1–13, 2012.
- [44] Hebertt Sira-Ramirez. On the linear control of the quad-rotor system. In *Proceedings of the 2011 American Control Conference*, pages 3178–3183, 2011.
- [45] Hebertt Sira-Ramirez and Sunil K Agrawal. *Differentially flat systems*. CRC Press, 2004.
- [46] Adam W. Strzebonski. Cylindrical Algebraic Decomposition using validated numerics. *Journal of Symbolic Computation*, 41(9):1021–1038, 2006.
- [47] Fajar Suryawan, José De Dona, and Maria Seron. Splines and polynomial tools for flatness-based constrained motion planning. *International Journal of Systems Science*, 43(8):1396–1411, 2012.
- [48] Alfred Tarski. A decision method for elementary algebra and geometry. In *Quantifier elimination and cylindrical algebraic decomposition*, pages 24–84. Springer, 1998.
- [49] Didier Theilliol, Cédric Join, Youmin Zhang, Didier Theilliol, Cédric Join, and Youmin Zhang. Actuator fault-tolerant control design based on reconfigurable reference input. *International Journal of Applied Mathematics and Computer Science, De Gruyter*, 18(4):553–560, 2008.
- [50] Jorge Villagra, Brigitte D Andréa-novel, Michel Fliess, Hugues Mounier, Jorge Villagra, Brigitte D Andréa-novel, Michel Fliess, Hugues Mounier Robust, Jorge Villagra, Brigitte Andr, Michel Fliess, and Hugues Mounier. Robust grey-box closed-loop stop-and-go control To cite this version : HAL Id : inria-00319591 Robust grey-box closed-loop stop-and-go control. 2008.
- [51] Johannes von Löwis and Joachim Rudolph. Real-time trajectory generation for flat systems with constraints. In *Nonlinear and Adaptive Control*, pages 385–394. 2002.

- [52] David J. Wilson, Russell J. Bradford, James H. Davenport, and Matthew England. Cylindrical Algebraic Sub-Decompositions. *Mathematics in Computer Science*, 8(2):263–288, 2014.
- [53] Jing Yu, Zhihao Cai, and Yingxun Wang. Minimum jerk trajectory generation of a quadrotor based on the differential flatness. In *Proceedings of 2014 IEEE Chinese Guidance, Navigation and Control Conference*, pages 832–837. IEEE, 2014.